NOYAUX DISCONTINUS ET MÉTHODES SANS MAILLAGE EN HYDRODYNAMIQUE

par

Philippe BELLEY

mémoire présenté au Département d'informatique
en vue de l'obtention du grade de maître ès sciences (M.Sc.)

FACULTÉ DES SCIENCES
UNIVERSITÉ DE SHERBROOKE

Sherbrooke, Québec, Canada, novembre 2007

III-1823

Library and Archives Canada

Published Heritage Branch

395 Wellington Street
Ottawa ON K1A 0N4
Canada

Bibliothèque et Archives Canada

Direction du Patrimoine de l'édition

395, rue Wellington
Ottawa ON K1A 0N4
Canada

Your file Votre référence
ISBN: 978-0-494-53145-7
Our file Notre référence
ISBN: 978-0-494-53145-7

NOTICE:

The author has granted a non-exclusive license allowing Library and Archives Canada to reproduce, publish, archive, preserve, conserve, communicate to the public by telecommunication or on the Internet, loan, distribute and sell theses worldwide, for commercial or non-commercial purposes, in microform, paper, electronic and/or any other formats.

The author retains copyright ownership and moral rights in this thesis. Neither the thesis nor substantial extracts from it may be printed or otherwise reproduced without the author's permission.

AVIS:

L'auteur a accordé une licence non exclusive permettant à la Bibliothèque et Archives Canada de reproduire, publier, archiver, sauvegarder, conserver, transmettre au public par télécommunication ou par l'Internet, prêter, distribuer et vendre des thèses partout dans le monde, à des fins commerciales ou autres, sur support microforme, papier, électronique et/ou autres formats.

L'auteur conserve la propriété du droit d'auteur et des droits moraux qui protège cette thèse. Ni la thèse ni des extraits substantiels de celle-ci ne doivent être imprimés ou autrement reproduits sans son autorisation.

In compliance with the Canadian Privacy Act some supporting forms may have been removed from this thesis.

While these forms may be included in the document page count, their removal does not represent any loss of content from the thesis.

Conformément à la loi canadienne sur la protection de la vie privée, quelques formulaires secondaires ont été enlevés de cette thèse.

Bien que ces formulaires aient inclus dans la pagination, il n'y aura aucun contenu manquant.

Canada

Le 11 janvier 2008

le jury a accepté le mémoire de M. Philippe Belley dans sa version finale.

Membres du jury

M. Richard Egli
Directeur
Département d'informatique

M. Fabrice Colin
Codirecteur
Université Laurentienne - Département de Mathématiques et d'informatique

M. Jean-Pierre Dussault
Membre
Département d'informatique

M. Ernest Monga
Président-rapporteur
Département de mathématiques

SOMMAIRE

Nous développons de nouvelles méthodes pour estimer la valeur d'une fonction, ainsi que les valeurs de ses dérivées première et seconde en un point quelconque. Ces méthodes reposent sur la convolution de la fonction avec de nouveaux noyaux discontinus à support fini, introduits dans ce mémoire. Notre approche, qui s'inspire des techniques sans maillage de l'hydrodynamique des particules lisses (ou «*smoothed particle hydrodynamics*», SPH), a l'avantage de permettre l'emploi d'approximations polynomiales et de certaines formules Newton-Cotes (comme les règles du trapèze et de Simpson) dans l'évaluation des convolutions. De plus, nous obtenons des bornes d'erreurs associées aux techniques SPH. Dans nos calculs numériques nous avons obtenu, grâce à la convolution avec nos noyaux discontinus, des résultats supérieurs à ceux obtenus par la convolution avec un noyau continu souvent utilisé en SPH classique (plus précisément, le noyau connu sous le nom de *poly6*). Cette supériorité est particulièrement évidente lorsque le support du noyau est petit.

REMERCIEMENTS

Mes plus vifs remerciements vont à l'endroit de Monsieur Richard Egli, mon directeur de recherche, et Monsieur Fabrice Colin, mon codirecteur, pour leurs encouragements, les précieux conseils qu'ils m'ont prodigués ainsi que pour leur soutien tout au long de la maîtrise.

TABLE DES MATIÈRES

FIGURES

INTRODUCTION

L'hydrodynamique des particules lisses (ou <<*smoothed particle hydrodynamics*>>, SPH) est une méthode sans maillage développée par Lucy [LUCY77] et par Gingold et Monaghan [GING77] pour résoudre les équations aux dérivées partielles rencontrées dans la simulation numérique de certains phénomènes astrophysiques. Cette méthode consiste à transformer, moyennant une convolution avec un noyau bien choisi (tel que défini dans [LIUL03a], par exemple), les équations de la physique des fluides afin de les rendre plus propices aux techniques d'analyse numérique. Le choix d'un noyau suffisamment lisse permet de transposer les opérations du gradient et du laplacien au noyau et ainsi de transformer le problème en un système d'équations différentielles ordinaires (par rapport au temps), puis en un système d'équations linéaires associé à un nombre fini de particules ([CAPU00], [ELLE02], [MULL03]). Cette façon originale d'aborder les problèmes d'astrophysique a ensuite été utilisée pour simuler les phénomènes fluides que l'on rencontre dans la vie courante ([CARL02], [ENRI02], [FOST01], [HINS02], [NIXO02], [SCHL99] et [STOR99]). L'efficacité de l'approche dépend non seulement du noyau, mais aussi de son gradient et de son laplacien. Or, dans la littérature, plusieurs noyaux sont proposés afin de permettre une bonne simulation des forces qui dépendent du gradient et du laplacien ([DESB96], [LIUL03b], [MULL03]). Cependant, plusieurs d'entre eux ne sont pas suffisamment différentiables pour justifier l'utilisation des identités de Green (c'est-à-dire, l'application des opérateurs gradient et laplacien au noyau). Conséquemment leur emploi peut laisser planer certains doutes. De plus, il n'existe dans la littérature que des résultats partiels ou des analyses a posteriori sur les bornes d'erreurs pour les approximations obtenues à l'aide des méthodes SPH classiques.

Dans ce mémoire nous aurons recours aux techniques propres à la théorie des fonctions généralisées, que nous allons appliquer à trois noyaux discontinus. Ils nous permettront d'utiliser les formules Newton-Cotes afin d'approximer les convolutions avec ces noyaux. De plus, nous utiliserons l'approximation polynomiale de Lagrange pour estimer la valeur d'une fonction en certains points. Lorsque comparée aux méthodes SPH classiques, cette approche nous permet d'obtenir, lorsque le support du noyau discontinu utilisé est petit, une grande amélioration dans les estimés des valeurs d'une fonction ainsi que de ses deux premières dérivées en un point. De plus, nous obtenons des bornes d'erreur pour notre méthode d'approximation qui, rappelons-le, s'inspire des techniques SPH.

Plus précisément, au chapitre 1 nous développerons la théorie de l'hydrodynamique des particules lisses afin de mieux comprendre l'importance des noyaux dans la solution de l'équation Navier-Stokes dans sa forme SPH. Nous donnerons ensuite quelques exemples de noyaux continus qui se sont avérés utiles en SPH et mentionnerons les difficultés que l'on rencontre lorsque ces noyaux ne sont pas continûment différentiables. Ensuite, nous introduirons pour un quelconque $h > 0$, trois noyaux discontinus avec un support donné par $[-h, h]$. Ces trois noyaux, notés $\delta_{[-h,h]}$, $\delta'_{[-h,h]}$ et $\delta''_{[-h,h]}$, sont à la base de ce mémoire.

Le chapitre 2 contient l'article de recherche axé sur nos trois noyaux discontinus. Pour un point x_0 quelconque et une fonction deux fois continûment différentiable f, nous approximons $f(x_0)$ par la convolution $\left(f * \delta_{[-h,h]}\right)(x_0)$. Ensuite, nous considérons une suite ordonnée de points $\{x_i\}_{i=1}^{N}$ et supposons que les valeurs de f ne sont connues qu'au points x_i pour tout indice $i = 1, ..., N$. Nous approximons ensuite la convolution $\left(f * \delta_{[-h,h]}\right)(x_0)$ par la règle du trapèze et montrons que l'erreur entre $f(x_0)$ et la somme obtenue par la règle du trapèze est d'ordre $O(h^2)$ lorsque $|x_i - x_{i-1}| < h$ pour tout $i = 2, ..., N$. Lorsque nous reproduisons les mêmes étapes mais avec un noyau continu (noté $k_{h,\text{poly6}}$ dans l'article) à la place de $\delta_{[-h,h]}$, nous obtenons des résultats numériques semblables à ceux que l'on rencontre en SPH classique et qui se retrouvent dans les tableaux: Table 1 - Table 5. Les résultats numériques dans les tableaux: Table 6 - Table 10, montrent la supériorité de $\delta_{[-h,h]}$ comparé à un noyau continu comme $k_{h,\text{poly6}}$ lorsque N et h sont petits. Nous arrivons aux mêmes conclusions lorsque, pour une fonction f trois (respectivement quatre) fois continûment différentiable, on approxime $f'(x_0)$ (respectivement $f''(x_0)$) par $\left(f * \delta'_{[-h,h]}\right)(x_0)$ (respectivement $\left(f * \delta''_{[-h,h]}\right)(x_0)$), que l'on approxime à son tour par la règle du trapèze (voir les tableaux: Table 11 - Table 20), ou mieux encore par la règle de Simpson dans le cas de la dérivée seconde (voir les tableaux: Table 21 - Table 25).

CHAPITRE 1

L'hydrodynamique des particules lisses (SPH)

Commençons par quelques rappels et définitions de base. Le vecteur position $\mathbf{r}(x, y, z)$ du point $(x, y, z) \in \mathbb{R}^3$ est défini par

$$\mathbf{r}(x, y, z) = x\overrightarrow{i} + y\overrightarrow{j} + z\overrightarrow{k}$$

où $\overrightarrow{i}$ désigne le vecteur dans $\mathbb{R}^3$ du point $(0, 0, 0)$ au point $(1, 0, 0)$, $\overrightarrow{j}$ celui de $(0, 0, 0)$ à $(0, 1, 0)$ et $\overrightarrow{k}$ celui de $(0, 0, 0)$ à $(0, 0, 1)$. La norme de $\mathbf{r}(x, y, z)$ est donnée par

$$\|\mathbf{r}(x, y, z)\| = \sqrt{x^2 + y^2 + z^2}.$$

Soit une représentation d'un fluide constitué de $N > 0$ particules aux positions $\mathbf{r}_j = x_j\overrightarrow{i} + y_j\overrightarrow{j} + z_j\overrightarrow{k}$ $(j = 1, ..., N)$ dans un domaine de $\mathbb{R}^3$. Nous écrirons $\mathbf{v}_j$ et $\mathbf{a}_j$ pour désigner respectivement le vecteur vitesse et le vecteur accélération de la particule à la position $\mathbf{r}_j$. Pour tout $h > 0$ assez petit, soit $k_h : \mathbb{R}^3 \to [0, \infty[$ un noyau tel que, pour toute position $\mathbf{r}_0 \in \mathbb{R}^3$ et toute fonction réelle continue f sur $\mathbb{R}^3$, l'on ait

$$\lim_{h \searrow 0} (f * k_h)(\mathbf{r}_0) = f(\mathbf{r}_0).$$

En SPH on cherche un bon noyau deux fois continûment différentiable k_h afin de simuler correctement le mouvement de ces particules, à partir de la formulation SPH de l'équation de Navier-Stokes [MULL03]

$$\mathbf{a}_i = -\sum_j m_j \frac{p_j}{\rho_i \rho_j} \boldsymbol{\nabla} k_h \left(\|\mathbf{r}_i - \mathbf{r}_j\|\right) + \mathbf{g} + \mu \sum_j m_j \frac{\mathbf{v}_j}{\rho_i \rho_j} \boldsymbol{\nabla}^2 k_h \left(\|\mathbf{r}_i - \mathbf{r}_j\|\right) \quad (1)$$

où

$$\begin{aligned}
\boldsymbol{\nabla} &= \frac{\partial}{\partial x}\overrightarrow{i} + \frac{\partial}{\partial y}\overrightarrow{j} + \frac{\partial}{\partial z}\overrightarrow{k} \\
\boldsymbol{\nabla}^2 &= \frac{\partial^2}{\partial x^2} + \frac{\partial^2}{\partial y^2} + \frac{\partial^2}{\partial z^2} \\
m_j &= \text{la masse de la particule à la position } \mathbf{r}_j \\
\rho_j &= \text{la densité à la position } \mathbf{r}_j \\
p_j &= \text{la pression à la position } \mathbf{r}_j \\
\mu &= \text{la viscosité} \\
\mathbf{g} &= \text{la somme des forces externes (telle que la gravité)} \\
\mathbf{r}_i - \mathbf{r}_j &= (x_i - x_j)\overrightarrow{i} + (y_i - y_j)\overrightarrow{j} + (z_i - z_j)\overrightarrow{k}.
\end{aligned}$$

Dans l'équation (1) l'accélération $\mathbf{a}_j$ dépend de trois forces. Le terme

$$\mathbf{f}_i^{\text{pression}} = -\sum_j m_j \frac{p_j}{\rho_j} \nabla k_h \left(\|\mathbf{r}_i - \mathbf{r}_j\|\right) \quad (2)$$

correspond à la force due à la pression (c.-à-d. dépend de ∇p_j),

$$\mathbf{f}_i^{\text{viscosité}} = \mu \sum_j m_j \frac{\mathbf{v}_j}{\rho_j} \nabla^2 k_h \left(\|\mathbf{r}_i - \mathbf{r}_j\|\right) \quad (3)$$

celle due à la viscosité (c.-à-d. dépend de $\nabla^2 \mathbf{v}_j$) et

$$\mathbf{f}_i^{\text{externe}} = \rho_i \mathbf{g} \quad (4)$$

celle due aux forces externes comme la gravité. La densité ρ_i à la position

$\mathbf{r}_i \in \mathbb{R}^3$ est approximée par

$$\rho_i \approx \sum_j m_j k_h (\|\mathbf{r}_i - \mathbf{r}_j\|) \tag{5}$$

et la pression $p(\mathbf{r})$ au point $\mathbf{r} \in \mathbb{R}^3$ est obtenue en fonction de la densité $\rho(\mathbf{r})$ en ce point via une équation d'état. (Voir par exemple [DOBR81] et [LIUL03a].) Dans le développement de la théorie, comme par exemple dans [MULL03], le gradient de p en $\mathbf{r}_i \in \mathbb{R}^3$ est estimé par

$$\nabla p_i \approx \sum_j p_j \frac{m_j}{\rho_j} \nabla k_h (\|\mathbf{r}_i - \mathbf{r}_j\|)$$

où $p_i = p(\mathbf{r}_i)$, et le laplacien de $\mathbf{v}$ en $\mathbf{r}_i$ est approximé par

$$\nabla^2 \mathbf{v}_i \approx \sum_j \mathbf{v}_j \frac{m_j}{\rho_j} \nabla^2 k_h (\|\mathbf{r}_i - \mathbf{r}_j\|)$$

où $\mathbf{v}_i = \mathbf{v}(\mathbf{r}_i)$.

De manière générale, si m_i est vu comme étant la masse totale d'un fluide occupant l'espace $U_i \subset \mathbb{R}^3$ (de volume $|U_i|$), alors $\rho_i = m_i / |U_i|$ et donc (5) devient

$$\rho_i \approx \sum_j \rho_j k_h (\|\mathbf{r}_i - \mathbf{r}_j\|) |U_j| \approx \int \rho(\mathbf{r}) k_h (\|\mathbf{r}_i - \mathbf{r}\|) \tag{6}$$

(où k_h est continu) tandis que

$$\nabla p_i \approx \sum_j p_j \nabla k_h (\mathbf{x}^i - \mathbf{x}^j) |U_j| \approx \int p(\mathbf{x}) \nabla k_h (\|\mathbf{r}_i - \mathbf{r}\|) \tag{7}$$

(où le noyau k_h est choisi continûment différentiable) et

$$\nabla^2 \mathbf{v}_i \approx \sum_j \mathbf{v}_j \nabla^2 k_h (\|\mathbf{r}_i - \mathbf{r}\|) |U_j| \approx \int \mathbf{v}(\mathbf{r}) \nabla^2 k_h (\|\mathbf{r}_i - \mathbf{r}\|) \tag{8}$$

(où le noyau k_h doit maintenant être deux fois continûment différentiable). Dans le cas unidimensionel, pour un point quelconque $x_0 \in \mathbb{R}$, une suite de points $\{x_j\}_{j=1}^{N} \subset \mathbb{R}$ et un noyau $k_h : \mathbb{R} \rightarrow [0, \infty[$ deux fois continûment différentiable, les équations (6)-(8) sont des cas particuliers d'approximations de $f(x_0)$, $f'(x_0)$ et $f''(x_0)$ en SPH classique par le biais des sommes

$$\begin{aligned}
\mathrm{cl}f(x_0) &= \sum_j \frac{m_j}{\rho_j} f(x_j)\, k_h(x_0 - x_j) \\
&\approx (f * k_h)(x_0) \\
&\approx \lim_{h \searrow 0} (f * k_h)(x_0) = f(x_0)\,,
\end{aligned}$$

$$\begin{aligned}
\mathrm{cl}f'(x_0) &= \sum_j \frac{m_j}{\rho_j} f(x_j)\, k_h'(x_0 - x_j) \\
&\approx (f * k_h')(x_0) \\
&= (f' * k_h)(x_0) \\
&\approx \lim_{h \searrow 0} (f' * k_h)(x_0) = f'(x_0)
\end{aligned}$$

et

$$\begin{aligned}
\mathrm{cl}f''(x_0) &= \sum_j \frac{m_j}{\rho_j} f(x_j)\, k_h''(x_0 - x_j) \\
&\approx (f * k_h'')(x_0) \\
&= (f'' * k_h)(x_0) \\
&\approx \lim_{h \searrow 0} (f'' * k_h)(x_0) = f''(x_0)
\end{aligned}$$

où la fonction $f : \mathbb{R} \rightarrow \mathbb{R}$ est continûment différentiable un nombre suffisant de fois.

1.1 Quelques noyaux continus

Dans la littérature on trouve plusieurs exemples de noyaux, chacun ayant ses avantages (voir, par exemple [MULL03]). Le noyau gaussien:

$$k_{h,\text{gauss}}(r) = \frac{1}{h\sqrt{\pi}} e^{-(r^2/h^2)}, \qquad r \in \mathbb{R}$$

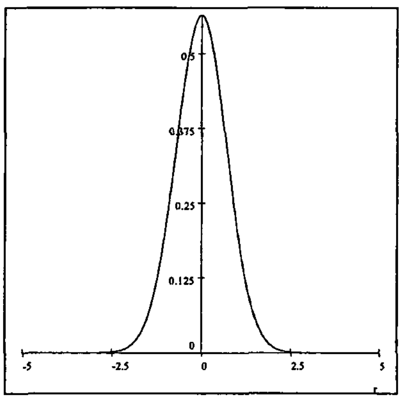

Figure 1: $k_{h,\text{gauss}}(r)$ pour $h = 1$

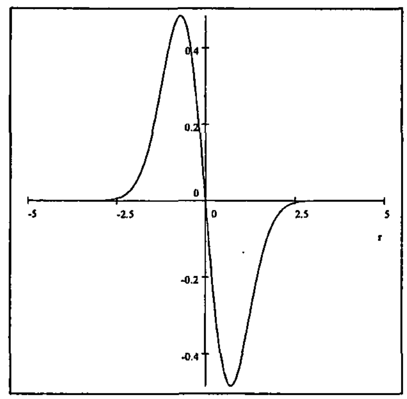

Figure 2: $k'_{h,\text{gauss}}(r)$ pour $h = 1$

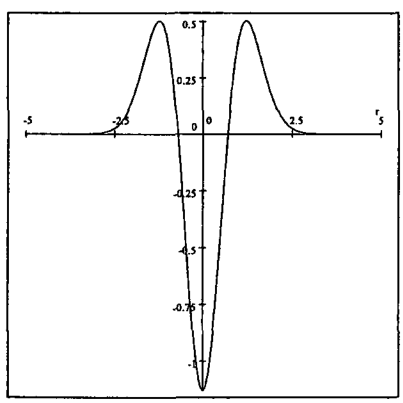

Figure 3: $k''_{h,\text{gauss}}(r)$ pour $h = 1$

a été utilisé dans [GING77] pour étudier les modèles stellaires en astrophysique. Ce noyau a été le premier à être utilisé en SPH. Il est lisse dans le sens qu'il est indéfiniment différentiable. De plus $k_{h,\text{gauss}}$ dépend de r^2 et non de r (qui comporte une racine carrée) et est utile pour calculer la densité

(5). Cependant, son support n'est pas borné et $k'_{h,\text{gauss}}$ comporte un terme en r. La grande variation dans les valeurs de $k_{h,\text{gauss}}$, $k'_{h,\text{gauss}}$ et $k''_{h,\text{gauss}}$ entraîne la nécessité de considérer un assez grand nombre de particules distribuées uniformément afin de garantir la qualité des résultats.

Le noyau polynomial:

$$k_{h,\text{poly6}}(r) = \frac{315}{64\pi h^9} \begin{cases} (h^2 - r^2)^3 & \text{si } -h \leq r \leq h \\ 0 & \text{autrement} \end{cases}$$

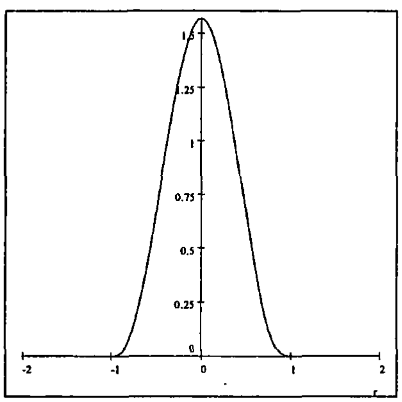

Figure 4: $k_{h,\text{poly6}}(r)$ pour $h = 1$

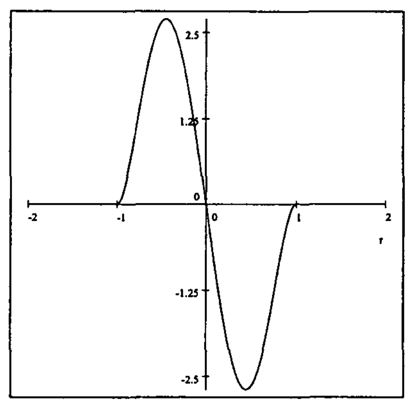

Figure 5: $k'_{h,\text{poly6}}(r)$ pour $h = 1$

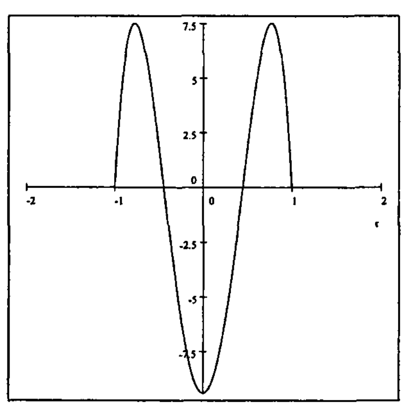

Figure 6: $k''_{h,\text{poly6}}(r)$ pour $h = 1$

a été introduit pour calculer la densité ρ_i. Ce noyau est deux fois continûment différentiable et, comme c'est le cas pour $k_{h,\text{gauss}}$, il est fonction de r^2 et non de r, ce qui le rend pratique pour calculer la densité ρ_i. De plus, son support est précisément le segment $-h \leq r \leq h$. La grande variation dans les valeurs de $k_{h,\text{poly6}}$, $k'_{h,\text{poly6}}$ et $k''_{h,\text{poly6}}$ sur $[-h, h]$ nécessite comme précédemment un assez grand nombre de particules distribuées uniformément.

Desbrun et Cani ont introduit dans [DESB96] un noyau un peu plus exotique, défini par

$$k_{h,\text{spiky}}(r) = \frac{15}{\pi h^6} \begin{cases} (h - |r|)^3 & \text{si } -h \leq r \leq h \\ 0 & \text{autrement.} \end{cases}$$

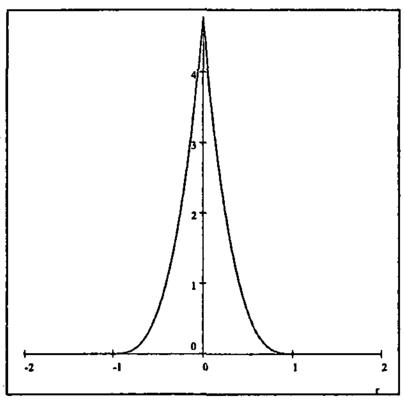

Figure 7: $k_{h,\text{spiky}}(r)$ pour $h = 1$

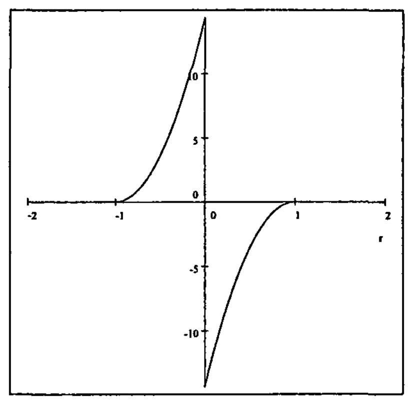

Figure 8: $k'_{h,\text{spiky}}(r)$ pour $h = 1$

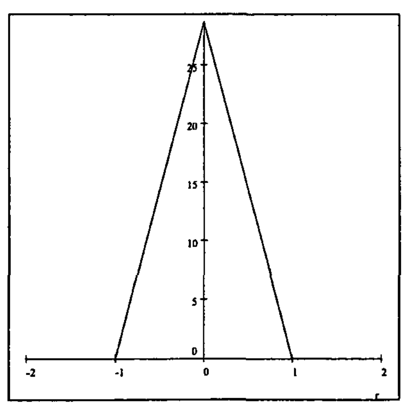

Figure 9: $k''_{h,\text{spiky}}(r)$ pour $h = 1$

Son support est précisément le segment $-h \leq r \leq h$. L'emploi de ce noyau dans le calcul des forces $\mathbf{f}_i^{\text{pression}}$ semble minimiser la formation d'amas grâce au fait que les valeurs de $k'_{h,\text{spiky}}(r)$ s'éloignent de 0 lorsque $r \to 0$. Cependant, il est fonction de r, ce qui exige le calcul d'une racine carrée, et donc le rend moins aisé à manipuler (ou à utiliser) que $k_{h,\text{gauss}}$ ou que $k_{h,\text{poly6}}$ dans le calcul de la densité ρ_i. De plus, $k'_{h,\text{spiky}}$ n'est pas défini à l'origine et $k''_{h,\text{spiky}}$ n'est donc pas approprié pour le calcul des forces $\mathbf{f}_i^{\text{viscosité}}$ puisque, pour ce noyau, la propriété

$$\int_{-h}^{h} \varphi(r)\, k''_{h,\text{spiky}}(r)\, dr = -\int_{-h}^{h} \varphi'(r)\, k'_{h,\text{spiky}}(r)\, dr,$$

qui est nécessaire pour obtenir la formulation faible de l'équation de Navier-Stokes (1), n'est pas vérifiée en général pour une fonction φ deux fois continûment différentiable. En effet, puisque $k'_{h,\text{spiky}}(-h) = k'_{h,\text{spiky}}(h) = 0$ (mais que $k'_{h,\text{spiky}}(0-) \neq k'_{h,\text{spiky}}(0+)$ pour la dérivée de $k_{h,\text{spiky}}$ à gauche et à droite en $r = 0$), on obtient en intégrant par parties

$$\begin{aligned}
\int_{-h}^{h} \varphi(r)\, k''_{h,\text{spiky}}(r)\, dr &= \int_{-h}^{0-} \varphi(r)\, k''_{h,\text{spiky}}(r)\, dr + \int_{0+}^{h} \varphi(r)\, k''_{h,\text{spiky}}(r)\, dr \\
&= \varphi(r)\, k'_{h,\text{spiky}}(r)\, |_{r=-h}^{r=0-} - \int_{-h}^{0-} \varphi'(r)\, k'_{h,\text{spiky}}(r)\, dr \\
&\quad + \varphi(r)\, k'_{h,\text{spiky}}(r)\, |_{r=0+}^{r=h} - \int_{0+}^{h} \varphi'(r)\, k'_{h,\text{spiky}}(r)\, dr \\
&= \varphi(0)\left[k'_{h,\text{spiky}}(0-) - k'_{h,\text{spiky}}(0+)\right] \\
&\quad - \int_{-h}^{h} \varphi'(r)\, k'_{h,\text{spiky}}(r)\, dr \\
&\neq -\int_{-h}^{h} \varphi'(r)\, k'_{h,\text{spiky}}(r)\, dr.
\end{aligned}$$

Le problème se manifeste également en dimension deux ou trois car, pour obtenir (1) moyennant la *deuxième identité de Green*, il faut supposer que la fonction k_h est deux fois différentiable partout dans le disque D_h de rayon h

centré à l'origine afin d'avoir

$$\int\int_{D_h} \varphi \nabla^2 k_h \, dxdy = \int\int_{D_h} k_h \nabla^2 \varphi \, dxdy$$

pour toute fonction φ deux fois différentiable sur D_h. Mais $k_h = k_{h,\text{spiky}}$ n'est pas différentiable à l'origine.

Dans [MULL03] les auteurs ont tenté de résoudre les difficultés rencontrées dans la littérature concernant la simulation des forces $\mathbf{f}_i^{\text{viscosité}}$ en posant $k_h = k_{h,\text{viscosité}}$ où

$$k_{h,\text{viscosité}}(r) = \frac{15}{2\pi h^3} \begin{cases} \left| -\frac{r}{2h^3} + \frac{r^2}{h^2} + \frac{h}{2r} - 1 \right| & \text{si } -1 \leq r \leq 1 \\ 0 & \text{autrement.} \end{cases}$$

Mais on rencontre le même problème avec $k''_{h,\text{viscosité}}$ qu'avec $k''_{h,\text{spiky}}$ à propos de la validité des identités de Green.

1.2 Trois noyaux discontinus

Dans ce mémoire nous introduirons trois noyaux discontinus que nous utiliserons pour estimer une fonction f de même que ses dérivées première et seconde en un point. Pour simplifier les calculs, nous nous restreindrons au cas unidimensionel. Le premier noyau, que nous dénoterons $\delta_{[-h,h]}$ pour $h > 0$, est défini par

$$\delta_{[-h,h]}(x) = \begin{cases} 1/2h & \text{si } -h < x < h \\ 0 & \text{autrement.} \end{cases}$$

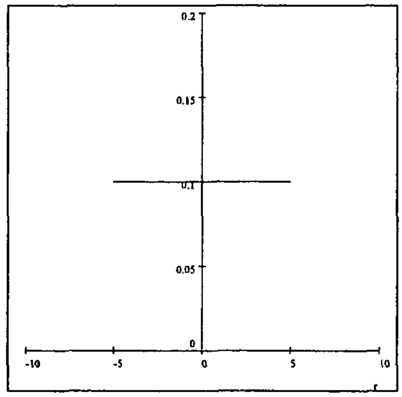

Figure 10: $\delta_{[-h,h]}(r)$ pour $h = 5$

Notre deuxième noyau, noté $\delta'_{[-h,h]}$, est défini par

$$\delta'_{[-h,h]}(x) = \begin{cases} 1/h^2 & \text{si } -h \leq x \leq 0 \\ -1/h^2 & \text{si } 0 < x \leq h \\ 0 & \text{autrement} \end{cases}$$

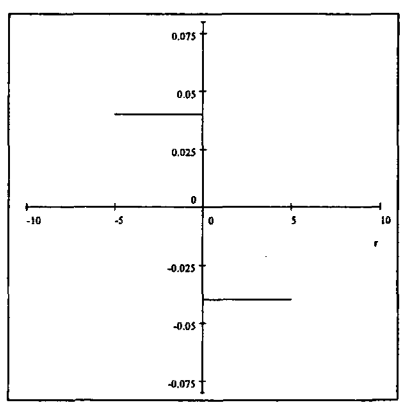

Figure 11: $\delta'_{[-h,h]}(r)$ pour $h = 5$

et le dernier, noté $\delta''_{[-h,h]}$, est défini par

$$\delta''_{[-h,h]}(x) = \begin{cases} 4/h^3 & \text{si } h/2 < |x| < h \\ -4/h^3 & \text{si } 0 \leq |x| < h/2 \\ 0 & \text{autrement.} \end{cases}$$

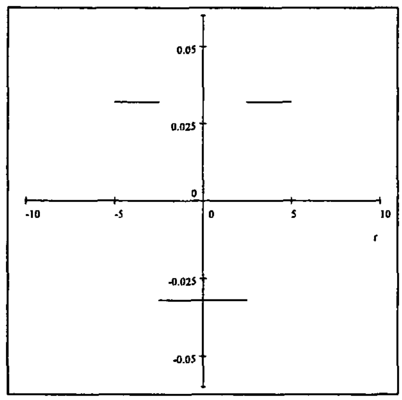

Figure 12: $\delta''_{[-h,h]}(r)$ pour $h = 5$

Ils seront utilisés, respectivement, pour approximer une fonction f et ses deux premières dérivées en un point, grâce à la convolution de ces noyaux avec f. Ces convolutions seront estimées par la règle du trapèze appliquée à l'approximation linéaire de f (obtenue à partir des valeurs connues $\{f(x_j)\}_{j=1}^{N}$). Ensuite nous améliorerons nos calculs numériques de la dérivée seconde en utilisant la règle de Simpson appliquée à l'approximation quadratique de f (à la place de la règle du trapèze appliquée à l'approximation linéaire).

CHAPITRE 2

Noyaux discontinus et bornes d'erreurs

Dans ce chapitre nous trouvons l'article ‹‹Non-Smooth Kernels for Mesh Free Methods in Fluid Dynamics›› que nous soumettrons à la revue *Computers & Mathematics with Applications.* On y trouve trois nouveaux noyaux qui servent à approximer, en un point donné, la valeur d'une fonction ainsi que de ses dérivées première et seconde. Ces noyaux vont nous permettre d'obtenir des bornes d'erreur pour des méthodes d'approximation qui s'inspirent des techniques SPH.

Ma contribution a d'abord consisté à avancer l'idée d'utiliser les noyaux discontinus $\delta_{[-h,h]}$, $\delta'_{[-h,h]}$ et $\delta''_{[-h,h]}$ plutôt que des noyaux continus. J'ai été amené ensuite à concevoir et mettre en oeuvre le programme utilisé pour les simulations numériques présentées dans l'article. Finalement, j'ai rédigé les sections 1, 2, 5 et 6 de l'article.

NON-SMOOTH KERNELS FOR MESH FREE METHODS IN FLUID DYNAMICS

J.-M.Belley[1], P. Belley[1], F. Colin[2,0], R. Egli[1,0]

[1]Faculté des sciences, Université de Sherbrooke, Sherbrooke (QC), Canada J1K2R1

[2]Department of Mathematics and Computer Science, Laurentian University, Sudbury (ON), Canada, P3E 2C6

Abstract

A function and its first two derivatives are estimated by convolutions with well chosen non-differentiable kernels. The convolutions are in turn approximated by Newton-Cotes integration techniques with the aid of a polynomial interpolation based on an arbitrary finite set of points. Precise numerical results are obtained with far fewer points than in classic SPH, and error bounds are derived.

1 Introduction

Smoothed particle hydrodynamics (SPH) was developed by Lucy [12] and by Gingold and Monaghan ([8], [13]) to simulate astrophysical phenomena in the absence of symmetry. It is a mesh free Lagrangian particle method which models fluid flow. In this paper, by SPH methods we mean the mesh free technique that mainly consists of transposing to a well chosen kernel the gradient and Laplacian operators encountered in a system of equations governing the motion of "fluid particles". When the kernel is continuously differentiable (a sufficient number of times), we can apply Green's identities

[0]Research funded in part by the Natural Sciences and Engineering Reaearch Council of Canada.

to justify these operations. The original problem is then transformed to that of a system of ordinary differential equations (with respect to time) which are then solved numerically ([3], [5], [14]). This original method of handling astrophysical problems has also been used to simulate fluid motion encountered in every day life ([4], [6], [7], [9], [15], [16]). With respect to numerical calculations, the effectiveness of this approach depends not only on the choice of the kernel, but also on its gradient and Laplacian. In the literature, several kernels are proposed to provide a good simulation of the component of the fluid flow due to pressure, which depends on the gradient, and of that due to viscosity, which depends on the Laplacian ([2], [11], [14]). Our purpose here is to apply the methods of generalized functions to well chosen non-differentiable kernels. In so doing, we provide a mathematically justifiable intuitive technique that improves the accuracy of the numerical calculations when the number of particles is low.

In SPH, we are given a finite number N of particles occupying positions $\{\mathbf{x}_i\}_{i=1}^{N} \subset \mathbb{R}^3$ and, for each $h > 0$, we choose a kernel $k_h : \mathbb{R}^3 \to [0, \infty[$ (preferably a twice continuously differentiable function of bounded support about the origin) such that, for any continuous function f, $\lim_{h \downarrow 0} (f * k_h)(x_0) = f(x_0)$ where $*$ denotes convolution. In the literature, if m_i $(i = 1, ..., N)$ designates the mass of the particle at position $\mathbf{x}_i$ then the density ρ_j at position $\mathbf{x}_j \in \mathbb{R}^3$ is approximated by

$$\rho_j \approx \sum_{i=1}^{N} m_i k_h (\mathbf{x}_j - \mathbf{x}_i) . \tag{1}$$

If m_i is viewed as the total mass of a fluid occupying the space $U_i \subset \mathbb{R}^3$ (of volume $|U_i|$), then $\rho_i = m_i / |U_i|$ and so (1) is equivalent to

$$\rho_j \approx \sum_{i=1}^{N} \rho_i k_h (\mathbf{x}_j - \mathbf{x}_i) |U_i| . \tag{2}$$

The gradient of the pressure field $p(\mathbf{x})$ at $\mathbf{x}_j$ is then approximated by

$$\nabla p_j \approx \sum_{i=1}^{N} p_i \frac{m_i}{\rho_i} \nabla k_h (\mathbf{x}_j - \mathbf{x}_i) = \sum_{i=1}^{N} p_i \nabla k_h (\mathbf{x}_j - \mathbf{x}_i) |U_i| \tag{3}$$

where k_h is chosen continuously differentiable and the pressure $p_i = p(\mathbf{x}_i)$ is obtained as a function of the density ρ_i by way of a state equation. Furthermore, the Laplacian of the velocity field $\mathbf{v}(\mathbf{x})$ at $\mathbf{x}_j$ is approximated by

$$\nabla^2 \mathbf{v}_j \approx \sum_{i=1}^{N} \mathbf{v}_i \frac{m_i}{\rho_i} \nabla^2 k_h(\mathbf{x}_j - \mathbf{x}_i) = \sum_{i=1}^{N} \mathbf{v}_i \nabla^2 k_h(\mathbf{x}_j - \mathbf{x}_i)|U_i| \tag{4}$$

where $\mathbf{v}_i = \mathbf{v}(\mathbf{x}_i)$ and k_h is chosen twice continuously differentiable. In SPH one seeks a kernel k_h and values for ρ_i that give a good approximation and accelerate calculations in (2)-(4).

In one dimension (or in terms of radial symmetry) the Gaussian kernel

$$k_{h,\text{gauss}}(x) = \frac{1}{h\sqrt{\pi}} e^{-x^2/h^2} \qquad x \in \mathbb{R} \tag{5}$$

was first used by Gingold and Monaghan [8] in the study of stellar formation. This kernel of unbounded support is smooth in the sense that it is infinitely differentiable. To calculate the density by means of (1), the kernel

$$k_{h,\text{poly6}}(x) = \frac{315}{64\pi h^9} \begin{cases} (h^2 - x^2)^3 & \text{if } -h \le x \le h \\ 0 & \text{otherwise} \end{cases} \tag{6}$$

was introduced in [14], while

$$k_{h,\text{spiky}}(x) = \frac{15}{\pi h^6} \begin{cases} (h - |x|)^3 & \text{if } -h \le x \le h \\ 0 & \text{otherwise} \end{cases} \tag{7}$$

was used in [2] to calculate (3). When normalized for $\mathbb{R}$, (6) becomes

$$k_{h,\text{poly6}}(x) = \frac{35}{32h^7} \begin{cases} (h^2 - x^2)^3 & \text{if } -h \le x \le h \\ 0 & \text{otherwise.} \end{cases} \tag{8}$$

In the one dimensional case, for any $x_0 \in \mathbb{R}$, (2)-(4) generalizes to

$$f(x_0) \approx \sum_{i=1}^{N} f(x_i) k_h(x_0 - x_i)|U_i| \approx (f * k_h)(x_0), \tag{9}$$

$$f'(x_0) \approx \sum_{i=1}^{N} f(x_i) k_h'(x_0 - x_i)|U_i| \approx (f * k_h')(x_0) \tag{10}$$

and

$$f''(x_0) \approx \sum_{i=1}^{N} f(x_i) k_h''(x_0 - x_i)|U_i| \approx (f * k_h'')(x_0) \tag{11}$$

whenever $f : \mathbb{R} \to \mathbb{R}$ and k_h are continuously differentiable a sufficient number of times and $*$ denotes the convolution operator. In this paper we propose discontinuous kernels in place of k_h, k'_h and k''_h in (9)-(11). The error in approximating $f(x_0)$, $f'(x_0)$ and $f''(x_0)$ by the corresponding convolution will be shown to be of order $O(h^2)$. The convolutions will in turn be estimated by Newton-Cotes integration formulas in conjunction with a polynomial interpolation obtained from the values of f at the points $\{x_i\}_{i=1}^N$. It will be shown that, when $|x_i - x_{i-1}| < h$ for all $i = 1, ..., N$, the error between the convolutions and the estimations is also of order $O(h^2)$.

2 Some natural discontinuous kernels on $\mathbb{R}$

For any interval $[a, b] \subset \mathbb{R}$, let $\delta_{[a,b]}$ be the discontinuous function on $\mathbb{R}$ defined by

$$\delta_{[a,b]}(x) = \begin{cases} 1/(b-a) & \text{if } a \le x \le b \\ 0 & \text{otherwise.} \end{cases} \tag{12}$$

Our first kernel is the function $\delta_{[-h,h]}$ for all $h > 0$. Clearly we have

$$\left. \begin{array}{l} \int_{-\infty}^{\infty} \delta_{[-h,h]}(x_0 - x)\, dx = 1, \\ \int_{-\infty}^{\infty} x\delta_{[-h,h]}(x_0 - x)\, dx = x_0, \\ \int_{-\infty}^{\infty} x^2\delta_{[-h,h]}(x_0 - x)\, dx = {x_0}^2 + h^2/3. \end{array} \right\} \tag{13}$$

The above conditions are often called *reproducing conditions* (see for example [10]) because, as we can see, the representation of a polynomial of first degree by a convolution involving this kernel and the polynomial is exact. Given $x_0 \in \mathbb{R}$ and given f in the class $C_h(x_0)$ of real functions on $\mathbb{R}$ which are continuous on some open interval containing $[x_0 - h, x_0 + h]$, we have the well-known identity

$$f(x_0) = \lim_{h \searrow 0} \left(f * \delta_{[-h,h]}\right)(x_0). \tag{14}$$

In this way, (14) defines the *generalized function* δ on $\mathbb{R}$ for which, in the sense of distributions,

$$f(x_0) = (f * \delta)(x_0)$$

for all $f \in C_h(x_0)$.

Remark 1. *In the one dimensional case, (1) with* $\delta_{[-h,h]}$ *in place of* k_h *becomes*

$$\rho_j \approx \sum_{i=1}^{N} m_i \delta_{[-h,h]} (\mathbf{x}_j - \mathbf{x}_i) \tag{15}$$

which, by virtue of (12), is the total mass in the segment $[x_0 - h, x_0 + h]$ *divided by its length. Thus, in the context of particle hydrodynamics,* $\delta_{[-h,h]}$ *is an intuitive kernel for estimating the (linear) density in the sense that the right hand side of (15) is precisely the average density in the segment* $[x_0 - h, x_0 + h]$ *centered at* x_0.

Our second kernel on $\mathbb{R}$ is given by

$$\delta'_{[-h,h]} (x) = \frac{1}{h} \delta_{[-h,0]} (x) - \frac{1}{h} \delta_{[0,h]} (x) \tag{16}$$

or equivalently

$$\delta'_{[-h,h]} (x) = \begin{cases} 1/h^2 & \text{if } -h \leq x \leq 0 \\ -1/h^2 & \text{if } 0 < x \leq h \\ 0 & \text{otherwise.} \end{cases}$$

It is easy to show that

$$\left.\begin{array}{l} \int_{-\infty}^{\infty} \delta'_{[-h,h]} (x_0 - x) \, dx = 0, \\ \int_{-\infty}^{\infty} x \delta'_{[-h,h]} (x_0 - x) \, dx = 1, \\ \int_{-\infty}^{\infty} x^2 \delta'_{[-h,h]} (x_0 - x) \, dx = 2x_0, \\ \int_{-\infty}^{\infty} x^3 \delta'_{[-h,h]} (x_0 - x) \, dx = 3{x_0}^2 + h^2/2. \end{array}\right\} \tag{17}$$

Remark 2. *The approximations in (10) for continuously differentiable f and* k_h *come from*

$$f' (x_0) = \lim_{h \searrow 0} (f' * k_h) (x_0) = \lim_{h \searrow 0} (f * k'_h) (x_0) . \tag{18}$$

Now, if we define the continuous kernel k_h *to be*

$$k_h (x) = \begin{cases} (h + x) / h^2 & \textit{if } -h \leq x \leq 0 \\ (h - x) / h^2 & \textit{if } 0 \leq x \leq h \\ 0 & \textit{otherwise} \end{cases} \tag{19}$$

then

$$\delta'_{[-h,h]} (x) = \frac{\frac{d}{dx} k_h (x+) + \frac{d}{dx} k_h (x-)}{2}$$

at all points x, where $dk_h(x+)/dx$ is the derivative of $k_h(x)$ from the left and $dk_h(x-)/dx$ is the one from the right. Heuristically, $\delta'_{[-h,h]}$ can be viewed as the derivative k'_h of (19). Since k'_h is discontinuous, this approach presents mathematical difficulties when trying to justify (18) by way of $f' * k_h = f * k'_h$. For this reason we prefer to simply introduce $\delta'_{[-h,h]}$ as defined by (16) and show in what follows that (17) allows us to approximate the derivative of a differentiable function f by means of $f * \delta'_{[-h,h]}$. A similar remark can be made for the kernel that follows.

Our third kernel is defined by

$$\delta''_{[-h,h]}(x) = \frac{2}{h^2}\delta_{[-h,-h/2]}(x) - \frac{4}{h^2}\delta_{[-h/2,h/2]}(x) + \frac{2}{h^2}\delta_{[h/2,h]}(x) \tag{20}$$

or equivalently

$$\delta''_{[-h,h]}(x) = \begin{cases} 4/h^3 & \text{if } h/2 < |x| < h \\ -4/h^3 & \text{if } 0 \leq |x| < h/2 \\ 0 & \text{otherwise.} \end{cases}$$

We can easily show that

$$\left.\begin{array}{l} \int_{-\infty}^{\infty} \delta''_{[-h,h]}(x_0 - x)\ dx = 0, \\ \int_{-\infty}^{\infty} x\delta''_{[-h,h]}(x_0 - x)\ dx = 0, \\ \int_{-\infty}^{\infty} x^2\delta''_{[-h,h]}(x_0 - x)\ dx = 2, \\ \int_{-\infty}^{\infty} x^3\delta''_{[-h,h]}(x_0 - x)\ dx = 6x_0, \\ \int_{-\infty}^{\infty} x^4\delta''_{[-h,h]}(x_0 - x)\ dx = 12{x_0}^2 + 3h^2/2. \end{array}\right\} \tag{21}$$

3 A justification for $\delta_{[-h,h]}, \delta'_{[-h,h]}$ and $\delta''_{[-h,h]}$

Given $x_0 \in \mathbb{R}$, let f lie in the class $C^2_h(x_0)$ of real valued functions on $\mathbb{R}$ which are twice continuously differentiable in an open interval containing $[x_0 - h, x_0 + h]$. Then, for $x \in [x_0 - h, x_0 + h]$, we have by Taylor's theorem

$$f(x) = f(x_0) + f'(x_0)(x - x_0) + f''(\overline{x})\frac{(x - x_0)^2}{2} \tag{22}$$

for some $\overline{x}$ between x and x_0. Thus, for $h > 0$ small enough for (22) to hold, we have

$$\begin{aligned}
&\left(f * \delta_{[-h,h]}\right)(x_0) \\
&= \int f(x)\, \delta_{[-h,h]}(x_0 - x)\, dx \\
&= \int \left(f(x_0) + f'(x_0)(x - x_0) + f''(\overline{x})\frac{(x-x_0)^2}{2} \right) \delta_{[-h,h]}(x_0 - x)\, dx
\end{aligned}$$

and so, by (13),

$$\left|f(x_0) - \left(f * \delta_{[-h,h]}\right)(x_0)\right| = O\left(h^2\right) \quad \forall f \in C_h^2(x_0) \tag{23}$$

since an upper bound for the right-hand term is given by

$$\frac{h^2}{6} \sup_{\gamma \in (x_0 - h, x_0 + h)} |f''(\gamma)|.$$

Furthermore, (22) and (17) in conjunction with

$$\left| \int f''(\overline{x}) \frac{(x-x_0)^2}{2} \delta'_{[-h,h]}(x_0 - x) dx \right| \leq h \sup_{\gamma \in (x_0 - h, x_0 + h)} |f''(\gamma)|$$

yields

$$\left|f'(x_0) - \left(f * \delta'_{[-h,h]}\right)(x_0)\right| = O(h) \quad \forall f \in C_h^2(x_0). \tag{24}$$

As for the second derivative, it is possible to prove that $\left(f * \delta''_{[-h,h]}\right)(x_0)$ convergences to $f''(x_0)$ (as $h \downarrow 0$) by virtue of the fact that $f \in C_h^2(x_0)$ implies that f'' in (22) is uniformly continuous on the interval $[x_0 - h, x_0 + h]$. If we want a precise order of convergence for $\left(f * \delta''_{[-h,h]}\right)(x_0)$ we must add an additional regularity assumption on f. For example, f'' is α-Hölder continuous at x_0 (i.e. $f \in C_h^{2,\alpha}(x_0)$) for some $\alpha \in]0, 1]$ if, by definition, there exists a constant $C > 0$ such that

$$|f''(x) - f''(x_0)| \leq C|x - x_0|^\alpha$$

for all x. Applying the reproducing conditions (21) to (22) for the case $f \in C_h^{2,\alpha}(x_0)$ we get

$$\begin{aligned}
\left|f''(x_0) - \left(f * \delta''_{[-h,h]}\right)(x_0)\right| &= \left| \int \left(f''(x_0) - f''(\overline{x})\right) \frac{(x-x_0)^2}{2} \delta''_{[-h,h]}(x_0 - x) dx \right| \\
&\leq 4Ch^\alpha \\
&= O(h^\alpha) \quad \forall f \in C_h^{2,\alpha}(x_0).
\end{aligned} \tag{25}$$

To obtain convergence results better than (24) we can, for instance, assume that f lies in the class $C_h^3(x_0)$ of real valued functions on $\mathbb{R}$ which are three times continuously differentiable in a open interval containing $[x_0 - h, x_0 + h]$. Then for $x \in [x_0 - h, x_0 + h]$ we have by Taylor's theorem

$$f(x) = f(x_0) + f'(x_0)(x - x_0) + f''(x_0)\frac{(x - x_0)^2}{2} + f'''(\overline{x})\frac{(x - x_0)^3}{6} \quad (26)$$

for some $\overline{x}$ between x and x_0. Thus, for $h > 0$ small enough for (26) to be valid, we have

$$\begin{aligned}&\left(f * \delta'_{[-h,h]}\right)(x_0)\\ &= \int \left(f(x_0) + f'(x_0)(x - x_0) + f''(x_0)\frac{(x - x_0)^2}{2} \right) \delta'_h (x_0 - x)\ dx\\ &+ \int f'''(\overline{x})\frac{(x - x_0)^3}{6}\delta'_{[-h,h]} (x_0 - x)\ dx\end{aligned}$$

and so, by (17),

$$\left|f'(x_0) - \left(f * \delta'_{[-h,h]}\right)(x_0)\right| \leq \frac{h^2}{12} \sup_{\gamma \in (x_0 - h, x_0 + h)} |f'''(\gamma)|$$

which implies that

$$\left|f'(x_0) - \left(f * \delta'_{[-h,h]}\right)(x_0)\right| = O\left(h^2\right) \quad \forall f \in C_h^3(x_0). \quad (27)$$

We can also obtain convergence results better than (25) by assuming that f lies in the class $C_h^4(x_0)$ of real valued functions on $\mathbb{R}$ which are four times continuously differentiable in an open interval containing $[x_0 - h, x_0 + h]$. Then for $x \in [x_0 - h, x_0 + h]$, we have by Taylor's theorem

$$\begin{aligned}f(x) &= f(x_0) + f'(x_0)(x - x_0) + f''(x_0)\frac{(x - x_0)^2}{2} \quad (28)\\ &+ f'''(x_0)\frac{(x - x_0)^3}{6} + f^{iv}(\overline{x})\frac{(x - x_0)^4}{24}\end{aligned}$$

for some $\overline{x}$ between x and x_0. Thus, for $h > 0$ small enough for (28) to hold, we have

$$\begin{aligned}&\left(f * \delta''_{[-h,h]}\right)(x_0)\\ &= \int \left(f(x_0) + f'(x_0)(x - x_0) + f''(x_0)\frac{(x - x_0)^2}{2} \right) \delta''_{[-h,h]} (x_0 - x)\ dx\\ &+ \int \left(f'''(x_0)\frac{(x - x_0)^3}{6} + f^{iv}(\overline{x})\frac{(x - x_0)^4}{24}\right) \delta''_{[-h,h]} (x_0 - x)\ dx\end{aligned}$$

and so, by (21),

$$\left|f''(x_0) - \left(f * \delta''_{[-h,h]}\right)(x_0)\right| \leq \frac{h^2}{16} \sup_{\gamma \in (x_0-h, x_0+h)} \left|f^{iv}(\gamma)\right|$$

from which we get

$$\left|f''(x_0) - \left(f * \delta''_{[-h,h]}\right)(x_0)\right| = O\left(h^2\right) \quad \forall f \in C_h^4(x_0). \tag{29}$$

4 Approximating $(f * \delta_{[a,b]})(x_0)$, $(f * \delta'_{[-h,h]})(x_0)$ and $(f * \delta''_{[-h,h]})(x_0)$ by sums

We have for all $f \in C_h(x_0)$,

$$\left(f * \delta_{[-h,h]}\right)(x_0) = \int_{x_0-h}^{x_0+h} f(x)\, \delta_{[-h,h]}(x_0 - x) = \frac{1}{2h} \int_{x_0-h}^{x_0+h} f(x)\, dx$$

and so $\left(f * \delta_{[-h,h]}\right)(x_0)$ can be approximated by any of the well known methods of numerical integration. In addition, we have

$$\left(f * \delta'_{[-h,h]}\right)(x_0) = \frac{1}{h^2}\left[\int_{x_0-h}^{x_0} f(x)\, dt - \int_{x_0}^{x_0+h} f(x)\, dt\right]$$

$$\left(f * \delta''_{[a,b]}\right)(x_0) = \frac{4}{h^3}\left[\int_{x_0-h}^{x_0-h/2} f(x)\, dt - \int_{x_0-h/2}^{x_0+h/2} f(x)\, dt + \int_{x_0+h/2}^{x_0+h} f(x)\, dt\right]$$

and so $(f * \delta'_{[-h,h]})(x_0)$ and $(f * \delta''_{[-h,h]})(x_0)$ can also be approximated by any of the well known methods of numerical integration. The following is the most elementary example of this approach.

4.1 The trapezoidal rule

Let $P(x_0, h) = \{x_i : i = 1, ..., n\}$ be a set of points in the closed interval $[x_0 - h, x_0 + h]$ such that

$$x_0 - h = x_1 < x_2 < \cdots < x_i < x_{i+1} < \cdots < x_{n-1} < x_n = x_0 + h \tag{30}$$

and define the sum

$$T(f, P(x_0, h)) = \frac{1}{2h} \sum_{i=1}^{n-1} \left(\frac{f(x_{i+1}) + f(x_i)}{2}\right)(x_{i+1} - x_i). \tag{31}$$

Then, by the well known error bound associated with the trapezoidal rule (see, for example, [1]) we have for all $f \in C_h^2(x_0)$

$$\left|\left(f * \delta_{[-h,h]}\right)(x_0) - T\left(f, P\left(x_0, h\right)\right)\right| \leq \frac{\left|P\left(x_0, h\right)\right|^2}{12} \sup_{\gamma \in (x_0 - h, x_0 + h)} |f''| \qquad (32)$$

where

$$\left|P\left(x_0, h\right)\right| = \sup\left\{\left|x^{i+1} - x^i\right| : i = 1, ..., n-1\right\}$$

and so

$$\begin{aligned}\left|\left(f * \delta_{[-h,h]}\right)(x_0) - T\left(f, P\left(x_0, h\right)\right)\right| &= O\left(\left|P\left(x_0, h\right)\right|^2\right) \\ &= O(h^2) \qquad \forall f \in C_h^2(x_0).\end{aligned}$$

The trapezoidal rule yields the following useful properties which are the counterparts of the reproducing conditions (13):

$$\left.\begin{array}{l} T\left(\delta_{[-h,h]}\left(x_0 - x\right), P\left(x_0, h\right)\right) = 1, \\ T\left(x\delta_{[-h,h]}\left(x_0 - x\right), P\left(x_0, h\right)\right) = x_0. \end{array}\right\} \qquad (33)$$

Now using Taylor's series expansion (22) along with (33) and (23), we get

$$\left|f(x_0) - T\left(f, P\left(x_0, h\right)\right)\right| = O\left(h^2\right) \quad \forall f \in C_h^2(x_0).$$

Remark 3. *In general the value of the function f is unknown at the points $x_0 \pm h$. To overcome this problem we can approximate $f(x_0 \pm h)$ by linear interpolation by way of the closest points on either side of $x_0 \pm h$ or by linearly extrapolating f by the two distinct points closest to $x_0 \pm h$ either inside or outside the interval $[x_0 - h, x_0 + h]$. In the latter case, if we take the closest points inside the interval $[x_0 - h, x_0 + h]$, we are assured of greater accuracy when using the trapezoidal rule, but we require at least two points (which is seldom a problem in SPH). In this paper we approximate $f(x_0 \pm h)$ by linear interpolation via the closest points on each side of $x_0 \pm h$.*

Given $P(x_0, h)$ ordered as in (30), we define

$$T'\left(f, P\left(x_0, h\right)\right) = \frac{2}{h}T\left(f, P\left(x_0 + \frac{h}{2}, \frac{h}{2}\right)\right) - \frac{2}{h}T\left(f, P\left(x_0 - \frac{h}{2}, \frac{h}{2}\right)\right) \qquad (34)$$

$$\begin{aligned} T''\left(f, P\left(x_0, h\right)\right) = &\frac{8}{h^2}\left(T\left(f, P\left(x_0 + \frac{3h}{4}, \frac{h}{4}\right)\right) + T\left(f, P\left(x_0 - \frac{3h}{4}, \frac{h}{4}\right)\right)\right) \\ &- \frac{8}{h^2}T\left(f, P\left(x_0, \frac{h}{2}\right)\right) \end{aligned} \qquad (35)$$

where $P\left(x_0+\frac{h}{2},\frac{h}{2}\right)$, $P\left(x_0-\frac{h}{2},\frac{h}{2}\right)$, $P\left(x_0+\frac{3h}{4},\frac{h}{4}\right)$, $P\left(x_0-\frac{3h}{4},\frac{h}{4}\right)$, and $P\left(x_0,\frac{h}{2}\right)$ consist, respectively, of the points of $P(x_0,h)$ in $[x_0,x_0+h]$, $[x_0-h,x_0]$, $[x_0+h/2,x_0+h]$, $[x_0-h,x_0-h/2]$, and $[x_0-h/2,x_0+h/2]$. It is then easy to show that these sums fulfill the reproducing conditions

$$\left.\begin{array}{l} T'\left(\delta'_{[-h,h]}\left(x_0-x\right),P\left(x_0,h\right)\right)=0 \\ T'\left(x\delta'_{[-h,h]}\left(x_0-x\right),P\left(x_0,h\right)\right)=1 \end{array}\right\} \tag{36}$$

and

$$\left.\begin{array}{l} T''\left(\delta''_{[-h,h]}\left(x_0-x\right),P\left(x_0,h\right)\right)=0 \\ T''\left(x\delta''_{[-h,h]}\left(x_0-x\right),P\left(x_0,h\right)\right)=0 \end{array}\right\} \tag{37}$$

which are respectively the analog of the reproducing conditions (17) and (21). Again by Taylor's series expansion (22) along with the reproducing conditions (36) and (37), and the estimates (24) and (25), we get

$$\begin{array}{l} \left|f'(x_0)-T'\left(f,P\left(x_0,h\right)\right)\right|=O\left(h\right) \quad \forall f\in C_h^2\left(x_0\right) \\ \left|f''(x_0)-T''\left(f,P\left(x_0,h\right)\right)\right|=O\left(h^{\alpha}\right) \quad \forall f\in C_h^{2,\alpha}\left(x_0\right),\ 0<\alpha\leq 1. \end{array}$$

4.2 A sum satisfying higher order consistency conditions

In this subsection, we will assume that we are dealing with smoother functions than those previously considered. To be more specific, we shall assume either $f\in C_h^3\left(x_0\right)$ or $f\in C_h^4\left(x_0\right)$. Recall that the partition $P\left(x_0,h\right)$ consists of n points $\{x_i\}_{i=1}^n\subset[x_0-h,x_0+h]$ ordered as in (30). Suppose for now that there exist $m,K\in\mathbb{N}\setminus\{0\}$ such that $n=Km+1$. If $\{I_k\}_{k=1}^K$ denotes the sequence of closed subintervals of $[x_0-h,x_0+h]$ given by

$$I_k=\left[x_{(k-1)m+1},x_{km+1}\right]$$

then each I_k contains $m+1$ consecutive points of $P\left(x_0,h\right)$. If $p_k(x)$ designates the unique interpolation polynomial (necessarily of degree no greater than m) for which $p_k(x)=f\left(x\right)$ at all points $x\in I_k\cap P\left(x_0,h\right)$, then the sum

$$S_m\left(f,P\left(x_0,h\right)\right)=\frac{1}{2h}\sum_{k=1}^{K}\int_{I_k}p_k(x)\,dx \tag{38}$$

approximates $\left(f * \delta_{[-h,h]}\right)(x_0)$. In particular $S_1\left(f, P\left(x_0, h\right)\right) = T\left(f, P\left(x_0, h\right)\right)$. Due to uniqueness of polynomial interpolation on a given set of points, the sum $S_m\left(f, P\left(x_0, h\right)\right)$, like the trapezoidal rule, is linear in f. But, if we are given m to begin with, the condition $n-1 = Km$ will generally not be satisfied for some $K \in \mathbb{N} \setminus \{0\}$. Nevertheless, there exists K such that there are $m+1$ consecutive points of $P\left(x_0, h\right)$ in I_k for $1 \leq k \leq K-1$ and no more than $m+1$ points in I_K. We can then borrow points from I_{K-1} in order to obtain the desired polynomial interpolation on I_K based on the last $m+1$ points of $P\left(x_0, h\right)$.

It is quite clear from our construction that the sum $S_m\left(f, P\left(x_0, h\right)\right)$ satisfies the reproducing conditions

$$\left.\begin{array}{l} S_m\left(\delta_{[-h,h]}\left(x_0 - x\right), P\left(x_0, h\right)\right) = 1, \\ S_m\left(x\delta_{[-h,h]}\left(x_0 - x\right), P\left(x_0, h\right)\right) = x_0. \end{array}\right\} \tag{39}$$

It is now possible to define $S_m{}'\left(f, P\left(x_0, h\right)\right)$ and $S_m{}''\left(f, P\left(x_0, h\right)\right)$ as we did $T'\left(f, P\left(x_0, h\right)\right)$ and $T''\left(f, P\left(x_0, h\right)\right)$ via (34) and (35). Moreover, we also have the reproducing conditions

$$\left.\begin{array}{l} S_m{}'\left(\delta'_{[-h,h]}\left(x_0 - x\right), P\left(x_0, h\right)\right) = 0 \\ S_m{}'\left(x\delta'_{[-h,h]}\left(x_0 - x\right), P\left(x_0, h\right)\right) = 1 \\ S_m{}'\left(x^2\delta'_{[-h,h]}\left(x_0 - x\right), P\left(x_0, h\right)\right) = 2x_0 \end{array}\right\} \tag{40}$$

and

$$\left.\begin{array}{l} S_m{}''\left(\delta''_{[-h,h]}\left(x_0 - x\right), P\left(x_0, h\right)\right) = 0 \\ S_m{}''\left(x\delta''_{[-h,h]}\left(x_0 - x\right), P\left(x_0, h\right)\right) = 0 \\ S_m{}''\left(x^2\delta''_{[-h,h]}\left(x_0 - x\right), P\left(x_0, h\right)\right) = 2 \\ S_m{}''\left(x^3\delta''_{[-h,h]}\left(x_0 - x\right), P\left(x_0, h\right)\right) = 6x_0. \end{array}\right\} \tag{41}$$

Thus, for any $f \in C_h^3\left(x_0\right)$ (respectively $f \in C_h^4\left(x_0\right)$), Taylor's series expansion (26) (respectively (28)) and the previous reproducing conditions (40) (respectively (41)) yield

$$\begin{array}{rcl} \left|\left(f * \delta'_{[-h,h]}\right)\left(x_0\right) - S_2{}'\left(f, P\left(x_0, h\right)\right)\right| &=& O(h^2) \quad \forall f \in C_h^3\left(x_0\right) \\ \left|\left(f * \delta''_{[-h,h]}\right)\left(x_0\right) - S_2{}''\left(f, P\left(x_0, h\right)\right)\right| &=& O(h) \quad \forall f \in C_h^3\left(x_0\right) \\ \left|\left(f * \delta''_{[-h,h]}\right)\left(x_0\right) - S_3{}''\left(f, P\left(x_0, h\right)\right)\right| &=& O(h^2) \quad \forall f \in C_h^4\left(x_0\right). \end{array}$$

Finally, using the estimates (27) and (29), we obtain

$$\begin{aligned}
|f'(x_0) - S_2{}'(f, P(x_0,h))| &= O(h^2), \quad \forall f \in C_h^3(x_0), \\
|f''(x_0) - S_2{}''(f, P(x_0,h))| &= O(h), \quad \forall f \in C_h^3(x_0), \\
|f''(x_0) - S_3{}''(f, P(x_0,h))| &= O(h^2), \quad \forall f \in C_h^4(x_0).
\end{aligned}$$

5 Numerical results

In what follows, we construct an ordered sequence of N points $\{x_i\}_{i=1}^N$ chosen at random (with uniform probability distribution) in $[-2, 2]$, and compare for different values of h (i.e. $h = 0.5, 0.25, 0.12, 0.06, 0.03, 0.01$) and for $N = 250$, 500, 1000, 2000 the average error in estimating by methods based on both old and new techniques of SPH, the values of the functions $f(x) = 2x + 5$, $f(x) = \sin(10\pi x)$, $f(x) = \sin(\pi x)$, $f(x) = x^2$ and $f(x) = \exp(x)$ at the points $x_i \in [-1, 1]$. First, for comparison with our new methods, we obtained numerical results using classic SPH with kernel (8). As is well known, acceptable errors are obtained in classic SPH provided we have a large number of points $\{x_i\}_{i=1}^N$. Otherwise the errors can be catastrophic for small N and h, as can be seen in Table 1-Table 5. We included these results so as to show in Table 6-Table 25 that SPH techniques based on our discontinuous kernels (12), (16) and (20) in conjunction with Newton-Cotes integration formulas, yield acceptable errors for these same small values of N and h as above. It may seem plausible that comparable results could be obtained by applying the Newton-Cotes integration formulas to any twice continuously differentiable kernel in place of our discontinuous kernels. This is false, as shown in Table 6-Table 25 where the numerical results derived from our discontinuous kernels are compared to those obtained by applying the same techniques to kernel (8).

5.1 Using classic SPH

In classic SPH, the approximations of $f(x_i)$, $f'(x_i)$ and $f''(x_i)$ with respect to a twice continuously differentiable kernel k_h, are given by the sums

$$\text{cl}f(x_i) = \sum_j \frac{m_j}{\rho_j} f(x_j)\, k_h(x_i - x_j),$$

$$\text{cl}f'(x_i) = \sum_j \frac{m_j}{\rho_j} f(x_j)\, k_h'(x_i - x_j)$$

and

$$\mathrm{cl}f''(x_i) = \sum_j \frac{m_j}{\rho_j} f(x_j)\, k_h''(x_i - x_j)$$

respectively, where m_i is the mass of the particle at point x_i and ρ_i, the density at the same point, is given by

$$\rho_i = \sum_j m_j k_h (x_i - x_j).$$

For each N, h and $x_i \in [-1, 1]$ we measured numerically the errors $\mathrm{cle}_{h,6}(f, x_i)$, $\mathrm{cle}'_{h,6}(f, x_i)$ and $\mathrm{cle}''_{h,6}(f, x_i)$ given by

$$\mathrm{cle}_{h,6}(f, x_i) = |f(x_i) - \mathrm{cl}f(x_i)|,$$

$$\mathrm{cle}'_{h,6}(f, x_i) = |f'(x_i) - \mathrm{cl}f'(x_i)|$$

and

$$\mathrm{cle}''_{h,6}(f, x_i) = |f''(x_i) - \mathrm{cl}f''(x_i)|$$

for $k_h = k_{h,\mathrm{poly6}}$ (defined by (8)) and $m_j = 1$ (for all j). We then took the average $\mathrm{cl}E_{h,6}$ of all $\mathrm{cle}_{h,6}(f, x_i)$, the average $\mathrm{cl}E'_{h,6}$ of all $\mathrm{cle}'_{h,6}(f, x_i)$ and the average $\mathrm{cl}E''_{h,6}$ of all $\mathrm{cle}''_{h,6}(f, x_i)$ for all $x_i \in [-1, 1]$. The results are found in Table 1-Table 5.

5.2 Using trapezoidal rule

For the functions f above and for each N, h and $x_i \in [-1, 1]$ we calculated the errors

$$e_{h,6}(f, x_i) = |f(x_i) - T_{h,6}(f, P(x_i, h))|$$

and

$$e_{h,\delta}(f, x_i) = \left|f(x_i) - T_{h,\delta}\left(\overline{f}, P(x_i, h)\right)\right|$$

where $P(x_i, h)$ is the set of all points of $\{x_j\}_{j=1}^{N}$ in $[x_i - h, x_i + h]$ augmented by $x_i \pm h$,

$$\begin{aligned} &T_{h,6}(f, P(x_i, h)) \\ &= f(x_m)\, k_{h,\mathrm{poly6}}(x_i - x_m)(x_m - (x_i - h))/2 \\ &+ \sum_{j=m}^{n-1} [f(x_j)\, k_{h,\mathrm{poly6}}(x_i - x_j) + f(x_{j+1})\, k_{h,6}(x_i - x_{j+1})](x_{j+1} - x_j)/2 \\ &+ f(x_n)\, k_{h,\mathrm{poly6}}(x_i - x_n)((x_i + h) - x_n)/2 \end{aligned}$$

	$N=2000$			$N=1000$		
h	$\mathrm{cl}E_{h,6}$	$\mathrm{cl}E'_{h,6}$	$\mathrm{cl}E''_{h,6}$	$\mathrm{cl}E_{h,6}$	$\mathrm{cl}E'_{h,6}$	$\mathrm{cl}E''_{h,6}$
0.50	0.06334	0.56937	4.5181	0.09730	0.78595	6.3623
0.25	0.08594	1.2466	21.726	0.11489	1.7116	29.899
0.12	0.09886	3.0268	108.85	0.13917	4.1362	144.90
0.06	0.14494	9.2762	673.98	0.23348	16.236	1133.9
0.03	0.19963	27.376	4355.6	0.30146	43.813	6412.3
0.01	0.32485	158.01	70293	0.35943	245.65	109625
	$N=500$			$N=250$		
h	$\mathrm{cl}E_{h,6}$	$\mathrm{cl}E'_{h,6}$	$\mathrm{cl}E''_{h,6}$	$\mathrm{cl}E_{h,6}$	$\mathrm{cl}E'_{h,6}$	$\mathrm{cl}E''_{h,6}$
0.50	0.15347	1.2541	10.334	0.36387	2.4518	18.983
0.25	0.17213	2.6623	52.424	0.25278	3.7328	51.313
0.12	0.28619	9.4018	301.02	0.23017	7.4677	260.53
0.06	0.30874	24.609	1728.1	0.29776	32.991	2480.4
0.03	0.39454	70.143	9835.4	0.35370	90.205	15543
0.01	0.20204	256.44	142887	0.12151	192.05	180851

Table 1: $\mathrm{cl}E_{h,6}$, $\mathrm{cl}E'_{h,6}$and $\mathrm{cl}E''_{h,6}$ in classic SPH for $f(x)=2x+5$

and

$$\begin{aligned} T_{h,\delta}\left(\overline{f}, P\left(x_i,h\right)\right) &= \left[f\left(x_m\right)+\overline{f}\left(x_i-h\right)\right]\left(x_m-\left(x_i-h\right)\right)/4h \\ &+\sum_{j=m}^{n-1}\left[f\left(x_j\right)+f\left(x_{j+1}\right)\right]\left(x_{j+1}-x_j\right)/4h \\ &+\left[f\left(x_n\right)+\overline{f}\left(x_i+h\right)\right]\left(\left(x_i+h\right)-x_n\right)/4h \end{aligned}$$

with

$$\overline{f}\left(x_i-h\right)=f\left(x_m\right)-\frac{f\left(x_m\right)-f(x_{m-1})}{x_m-x_{m-1}}\left(x_m-\left(x_i-h\right)\right)$$

and

$$\overline{f}\left(x_i+h\right)=f\left(x_n\right)+\frac{f\left(x_{n+1}\right)-f(x_n)}{x_{n+1}-x_n}\left(\left(x_i+h\right)-x_n\right)$$

where x_m is the first element of $\{x_j\}_{j=1}^{N}$ in $[x^i-h,x^i+h]$ and x_n is the last. We then took the average $E_{h,6}$ of all $e_{h,6}\left(f,x_i\right)$ and the average $E_{h,\delta}$ of all $e_{h,\delta}\left(f,x_i\right)$. The results are given in Table 6-Table 10.

	$N=2000$			$N=1000$		
h	$\mathrm{cl}E_{h,6}$	$\mathrm{cl}E'_{h,6}$	$\mathrm{cl}E''_{h,6}$	$\mathrm{cl}E_{h,6}$	$\mathrm{cl}E'_{h,6}$	$\mathrm{cl}E''_{h,6}$
0.50	0.63638	20.048	627.97	0.65533	19.669	651.43
0.25	0.64784	20.424	639.33	0.66786	20.059	663.99
0.12	0.36560	11.659	359.64	0.36062	11.165	357.41
0.06	0.11678	3.9630	134.65	0.10669	4.1896	164.47
0.03	0.03898	4.4517	563.04	0.04850	6.5385	842.24
0.01	0.04373	21.252	9043.4	0.05191	32.174	13569
	$N=500$			$N=250$		
h	$\mathrm{cl}E_{h,6}$	$\mathrm{cl}E'_{h,6}$	$\mathrm{cl}E''_{h,6}$	$\mathrm{cl}E_{h,6}$	$\mathrm{cl}E'_{h,6}$	$\mathrm{cl}E''_{h,6}$
0.50	0.63797	19.514	655.97	0.65512	19.109	662.45
0.25	0.63892	19.929	667.04	0.65482	19.543	672.72
0.12	0.34136	11.374	357.75	0.33447	11.363	339.87
0.06	0.10605	5.8738	221.34	0.10315	7.3790	287.25
0.03	0.06522	10.890	1328.0	0.06649	13.693	1722.6
0.01	0.03560	37.362	18460	0.02188	33.785	24052

Table 2: $\mathrm{cl}E_{h,6}$, $\mathrm{cl}E'_{h,6}$ and $\mathrm{cl}E''_{h,6}$ in classic SPH for $f(x)=\sin(10\pi x)$

Next we calculated the errors

$$e'_{h,6}(f,x_i)=\left|f'(x_i)-T'_{h,6}(f,P(x_i,h))\right|$$

and

$$e'_{h,\delta}(f,x_i)=\left|f'(x_i)-T'_{h,\delta}(f,P'(x_i,h))\right|$$

where $P'(x_i,h)$ is the set of all points of $\{x_i\}_{i=1}^{N}$ in $[x_i-h,x_i+h]$ augmented by $x_i\pm h$ (and so $P'(x_i,h)=P(x_i,h)$),

$$\begin{aligned}
&T'_{h,6}(f,P'(x_i,h))\\
&=f(x_m)\,k'_{h,\mathrm{pooly6}}(x_i-x_m)\,(x_m-(x_i-h))/2\\
&+\sum_{j=m}^{n-1}\left[f(x_j)\,k'_{h,\mathrm{poly6}}(x_i-x_j)+f(x_{j+1})\,k'_{h,\mathrm{poly6}}(x_i-x_{j+1})\right](x_{j+1}-x_j)/2\\
&+f(x_n)\,k'_{h,\mathrm{poly6}}(x_i-x_n)\,((x_i+h)-x_n)/2
\end{aligned}$$

where x_m and x_n are respectively the first and last points of $\{x_j\}_{j=1}^{N}$ in

	$N=2000$			$N=1000$		
h	$\mathrm{cl}E_{h,6}$	$\mathrm{cl}E'_{h,6}$	$\mathrm{cl}E''_{h,6}$	$\mathrm{cl}E_{h,6}$	$\mathrm{cl}E'_{h,6}$	$\mathrm{cl}E''_{h,6}$
0.50	0.08164	0.23033	0.92945	0.07827	0.18813	0.91038
0.25	0.02292	0.22139	3.6371	0.02275	0.23981	4.0089
0.12	0.01366	0.38487	14.630	0.01828	0.49429	18.882
0.06	0.01858	1.1575	88.021	0.02931	2.0094	138.89
0.03	0.02609	3.6291	584.99	0.03830	5.6103	873.57
0.01	0.04171	19.948	8554.2	0.04786	32.262	14173
	$N=500$			$N=250$		
h	$\mathrm{cl}E_{h,6}$	$\mathrm{cl}E'_{h,6}$	$\mathrm{cl}E''_{h,6}$	$\mathrm{cl}E_{h,6}$	$\mathrm{cl}E'_{h,6}$	$\mathrm{cl}E''_{h,6}$
0.50	0.07529	0.21708	1.2715	0.06020	0.24736	1.9444
0.25	0.02642	0.43426	7.9679	0.03442	0.46862	6.5698
0.12	0.03651	1.1454	41.076	0.03129	0.96801	38.962
0.06	0.04069	2.9824	223.23	0.04602	4.3273	325.45
0.03	0.05577	9.6304	1348.8	0.05440	12.975	2100.1
0.01	0.02925	35.330	19545	0.02017	29.722	26197

Table 3: $\mathrm{cl}E_{h,6}$, $\mathrm{cl}E'_{h,6}$ and $\mathrm{cl}E''_{h,6}$ in classic SPH for $f(x)=\sin(\pi x)$

$[x_i-h, x_i+h]$ and

$$\begin{aligned} T'_{h,\delta}\left(\overline{f}, P'(x_i,h)\right) &= \sum_{j=i}^{n-1}\left[f(x_j)+f(x_{j+1})\right](x_{j+1}-x_j)/2h^2 \\ &+ \left[f(x_n)+\overline{f}(x_i+h)\right]((x_i+h)-x_n)/2h^2 \\ &- \left[f(x_m)+\overline{f}(x_i-h)\right](x_m-(x_i-h))/2h^2 \\ &- \sum_{j=m}^{i-1}\left[f(x_j)+f(x_{j+1})\right](x_{j+1}-x_j)/2h^2 \end{aligned}$$

with

$$\overline{f}(x_i+h) = f(x_n) + \frac{f(x_{n+1})-f(x_n)}{x_{n+1}-x_n}\left[(x_i+h)-x_n\right]$$

and

$$\overline{f}(x_i-h) = f(x_m) - \frac{f(x_m)-f(x_{m-1})}{x_m-x_{m-1}}\left[x_m-(x_i-h)\right].$$

We then took the average $E'_{h,6}$ of all $e'_{h,6}(f,x_i)$ and the average $E'_{h,\delta}$ of all

	$N=2000$			$N=1000$		
h	$\mathrm{cl}E_{h,6}$	$\mathrm{cl}E'_{h,6}$	$\mathrm{cl}E''_{h,6}$	$\mathrm{cl}E_{h,6}$	$\mathrm{cl}E'_{h,6}$	$\mathrm{cl}E''_{h,6}$
0.50	0.02815	0.04582	0.37081	0.02815	0.05782	0.50829
0.25	0.01098	0.10459	1.6687	0.01349	0.15578	2.2812
0.12	0.00732	0.21517	8.0680	0.00863	0.25802	8.4689
0.06	0.01216	0.80745	55.183	0.01660	1.1773	81.021
0.03	0.01483	2.0087	303.01	0.02045	3.0051	419.72
0.01	0.02274	10.925	4882.0	0.02501	16.750	7266.6
	$N=500$			$N=250$		
h	$\mathrm{cl}E_{h,6}$	$\mathrm{cl}E'_{h,6}$	$\mathrm{cl}E''_{h,6}$	$\mathrm{cl}E_{h,6}$	$\mathrm{cl}E'_{h,6}$	$\mathrm{cl}E''_{h,6}$
0.50	0.02929	0.08598	0.81158	0.03766	0.19679	1.5385
0.25	0.01344	0.18031	3.1379	0.01933	0.21296	2.9291
0.12	0.01704	0.65781	22.020	0.01181	0.45869	17.543
0.06	0.02369	1.5615	115.35	0.01778	2.1412	180.60
0.03	0.02575	4.3052	598.17	0.02003	5.2929	956.10
0.01	0.01231	15.802	10256	0.00571	9.8614	11455

Table 4: $\mathrm{cl}E_{h,6}$, $\mathrm{cl}E'_{h,6}$ and $\mathrm{cl}E''_{h,6}$ in classic SPH for $f(x)=x^2$

$e'_{h,\delta}(f,x_i)$ as a measure of the error in approximating f' by $T'_{h,6}$ and $T'_{h,\delta}$ respectively. The results, are given in Table 11-Table 15.

We also calculated the errors

$$e''_{h,6}(f,x_i)=\left|f''(x_i)-T''_{h,6}(f,P(x_i,h))\right|$$

and

$$e''_{h,\delta}(f,x_i)=\left|f''(x_i)-T''_{h,\delta}(f,P''(x_i,h))\right|$$

where $P''(x_i,h)$ is the set of all points of $\{x_i\}_{i=1}^{N}$ in $[x_i-h,x_i+h]$ augmented by $x_i\pm h$ and $x_i\pm h/2$,

$$\begin{aligned}&T''_{h,6}(f,P(x_i,h))\\&=f(x_m)\,k''_{h,\text{poly6}}(x_i-x_m)(x_m-(x_i-h))/2\\&+\sum_{j=m}^{n-1}\left[f(x_j)\,k''_{h,\text{poly6}}(x_i-x_j)+f(x_{j+1})\,k''_{h,6}(x_i-x_{j+1})\right](x_{j+1}-x_j)/2\\&+f(x_n)\,k''_{h,\text{poly6}}(x_i-x_n)((x_i+h)-x_n)/2\end{aligned}$$

	$N = 2000$			$N = 1000$		
h	$\mathrm{cl}E_{h,6}$	$\mathrm{cl}E'_{h,6}$	$\mathrm{cl}E''_{h,6}$	$\mathrm{cl}E_{h,6}$	$\mathrm{cl}E'_{h,6}$	$\mathrm{cl}E''_{h,6}$
0.50	0.01859	0.15234	1.1641	0.02516	0.21077	1.6825
0.25	0.01880	0.28569	4.8171	0.02911	0.43754	7.2151
0.12	0.02193	0.72091	25.624	0.03273	1.0157	33.318
0.06	0.03428	2.1445	157.01	0.05672	3.9492	277.20
0.03	0.04653	6.4391	1026.4	0.07041	10.298	1476.9
0.01	0.07518	36.383	16535	0.08562	56.782	25460
	$N = 500$			$N = 250$		
h	$\mathrm{cl}E_{h,6}$	$\mathrm{cl}E'_{h,6}$	$\mathrm{cl}E''_{h,6}$	$\mathrm{cl}E_{h,6}$	$\mathrm{cl}E'_{h,6}$	$\mathrm{cl}E''_{h,6}$
0,50	0.03881	0.33477	2.7180	0.08594	0.58379	4.4095
0.25	0.04269	0.64195	11.883	0.05730	0.84537	11.129
0.12	0.06886	2.4025	71.903	0.05047	1.7230	56.769
0.06	0.07361	5.8303	412.46	0.06768	7.3782	581.76
0.03	0.08902	15.774	2225.0	0.07576	20.715	3651.0
0.01	0.04564	57.381	32259	0.02438	40.975	40705

Table 5: $\mathrm{cl}E_{h,6}$, $\mathrm{cl}E'_{h,6}$ and $\mathrm{cl}E''_{h,6}$ in classic SPH for $f(x) = \exp(x)$

	$N = 2000$		$N = 1000$		$N = 500$		$N = 250$	
h	$E_{h,6}$	$E_{h,\delta}$	$E_{h,6}$	$E_{h,\delta}$	$E_{h,6}$	$E_{h,\delta}$	$E_{h,6}$	$E_{h,\delta}$
.50	.00005	2e-15	.00021	2e-15	.00063	1e-15	.00696	1e-15
.25	.00016	2e-15	.00096	1e-15	.00368	8e-16	.03708	5e-16
.12	.00103	1e-15	.00666	1e-15	.03333	1e-15	.08569	8e-16
.06	.00431	3e-15	.02224	3e-15	.10255	3e-15	.17801	2e-15
.03	.02297	3e-15	.07107	4e-15	.17228	4e-15	.28514	4e-15
.01	.13674	4e-15	.24679	4e-15	.34626	4e-15	.42161	4e-15

Table 6: $E_{h,6}$ and $E_{h,\delta}$ for $f(x) = 2x + 5$

	$N = 2000$		$N = 1000$		$N = 500$		$N = 250$	
h	$E_{h,6}$	$E_{h,\delta}$	$E_{h,6}$	$E_{h,\delta}$	$E_{h,6}$	$E_{h,\delta}$	$E_{h,6}$	$E_{h,\delta}$
.50	.63645	.63544	.62636	.62561	.60476	.60517	.59261	.59421
.25	.64827	.55464	.63781	.54622	.61493	.52898	.60140	.52423
.12	.36593	.73431	.36009	.72208	.34730	.69409	.32111	.67217
.06	.11567	.31534	.11314	.31179	.10765	.30685	.10244	.31008
.03	.03057	.09087	.02987	.09179	.03784	.09777	.05063	.11349
.01	.01868	.01134	.03388	.01319	.04563	.01814	.05438	.02818

Table 7: $E_{h,6}$ and $E_{h,\delta}$ for $f(x) = \sin(10\pi x)$

	$N = 2000$		$N = 1000$		$N = 500$		$N = 250$	
h	$E_{h,6}$	$E_{h,\delta}$	$E_{h,6}$	$E_{h,\delta}$	$E_{h,6}$	$E_{h,\delta}$	$E_{h,6}$	$E_{h,\delta}$
.50	.08277	.23203	.08398	.23547	.08199	.22986	.08026	.22507
.25	.02158	.05881	.02188	.06462	.02130	.06320	.01979	.06237
.12	.00501	.01503	.00497	.01528	.00543	.01505	.01235	.01528
.06	.00133	.00378	.00237	.00387	.01317	.00391	.02466	.00432
.03	.00292	.00096	.00858	.00099	.02196	.00108	.03595	.00140
.01	.01824	.00011	.03155	.00013	.04278	.00019	.05055	.00032

Table 8: $E_{h,6}$ and $E_{h,\delta}$ for $f(x) = \sin(\pi x)$

	$N = 2000$		$N = 1000$		$N = 500$		$N = 250$	
h	$E_{h,6}$	$E_{h,\delta}$	$E_{h,6}$	$E_{h,\delta}$	$E_{h,6}$	$E_{h,\delta}$	$E_{h,6}$	$E_{h,\delta}$
.50	.02778	.08334	.02777	.08335	.02775	.08339	.02775	.08360
.25	.00694	.02084	.00691	.02085	.00693	.02089	.00837	.02108
.12	.00161	.00480	.00194	.00481	.00352	.00486	.00750	.00501
.06	.00053	.00120	.00230	.00121	.00707	.00125	.01061	.00139
.03	.00138	.00030	.00490	.00031	.01147	.00034	.01663	.00044
.01	.00916	.00004	.01612	.00004	.02327	.00006	.02834	.00010

Table 9: $E_{h,6}$ and $E_{h,\delta}$ for $f(x) = x^2$

	$N = 2000$		$N = 1000$		$N = 500$		$N = 250$	
h	$E_{h,6}$	$E_{h,\delta}$	$E_{h,6}$	$E_{h,\delta}$	$E_{h,6}$	$E_{h,\delta}$	$E_{h,6}$	$E_{h,\delta}$
.50	.01675	.05059	.01758	.05311	.01743	.05292	.01798	.05347
.25	.00417	.01253	.00430	.01316	.00437	.01314	.01213	.01337
.12	.00100	.00288	.00234	.00303	.00998	.00305	.02161	.00317
.06	.00102	.00072	.00630	.00076	.02732	.00079	.04422	.00087
.03	.00529	.00018	.01695	.00020	.04083	.00022	.06694	.00027
.01	.03142	.00002	.05761	.00003	.08255	.00004	.10094	.00006

Table 10: $E_{h,6}$ and $E_{h,\delta}$ for $f(x) = e^x$

	$N = 2000$		$N = 1000$		$N = 500$		$N = 250$	
h	$E'_{h,6}$	$E'_{h,\delta}$	$E'_{h,6}$	$E'_{h,\delta}$	$E'_{h,6}$	$E'_{h,\delta}$	$E'_{h,6}$	$E'_{h,\delta}$
.50	.00036	5e-15	.00178	3e-15	.00560	2e-15	.06120	2e-15
.25	.00320	7e-15	.01838	5e-15	.05639	3e-15	.53276	4e-15
.12	.03472	1e-14	.23474	1e-14	1.0807	1e-14	3.6529	9e-15
.06	.31072	2e-14	1.6165	2e-14	8.4953	2e-14	21.076	2e-14
.03	3.5035	3e-14	11.980	3e-14	36.918	2e-14	72.706	2e-14
.01	77.430	7e-14	179.59	6e-14	229.70	7e-14	229.06	8e-14

Table 11: $E'_{h,6}$ and $E'_{h,\delta}$ for $f(x) = 2x + 5$

	$N = 2000$		$N = 1000$		$N = 500$		$N = 250$	
h	$E'_{h,6}$	$E'_{h,\delta}$	$E'_{h,6}$	$E'_{h,\delta}$	$E'_{h,6}$	$E'_{h,\delta}$	$E'_{h,6}$	$E'_{h,\delta}$
.50	20.285	19.924	20.502	20.140	20.863	20.502	21.080	20.736
.25	20.662	19.596	20.884	19.811	21.260	20.174	21.563	20.401
.12	11.663	15.105	11.806	15.297	12.146	15.697	12.504	16.203
.06	3.7040	5.3546	3.9608	5.5002	5.147	5.9686	7.9410	7.0296
.03	1.3272	1.4871	2.7228	1.6181	6.969	2.1465	13.173	3.5428
.01	10.591	.23358	23.788	.45702	30.086	1.0699	30.336	2.5394

Table 12: $E'_{h,6}$ and $E'_{h,\delta}$ for $f(x) = \sin(10\pi x)$

	$N=2000$		$N=1000$		$N=500$		$N=250$	
h	$E'_{h,6}$	$E'_{h,\delta}$	$E'_{h,6}$	$E'_{h,\delta}$	$E'_{h,6}$	$E'_{h,\delta}$	$E'_{h,6}$	$E'_{h,\delta}$
.50	.25569	.37370	.25201	.36861	.25779	.37680	.27537	.39100
.25	.06656	.09936	.06546	.09804	.06999	.10059	.14290	.10730
.12	.01662	.02328	.02933	.02302	.13239	.02395	.54650	.02930
.06	.04180	.00586	.15901	.00586	1.0951	.00720	3.0543	.01498
.03	.46160	.00151	1.3124	.00176	4.8752	.00590	9.5777	.01893
.01	10.108	.00095	22.131	.00272	26.727	.00809	27.011	.02427

Table 13: $E'_{h,6}$ and $E'_{h,\delta}$ for $f(x) = \sin(\pi x)$

	$N=2000$		$N=1000$		$N=500$		$N=250$	
h	$E'_{h,6}$	$E'_{h,\delta}$	$E'_{h,6}$	$E'_{h,\delta}$	$E'_{h,6}$	$E'_{h,\delta}$	$E'_{h,6}$	$E'_{h,\delta}$
.50	.00003	.000002	.00022	.00001	.00057	.00003	.00618	.00031
.25	.00016	.000005	.00188	.00002	.00478	.00008	.04041	.00090
.12	.00217	.000012	.02310	.00007	.07748	.00028	.27295	.00173
.06	.01948	.000028	.14887	.00017	.54023	.00078	1.2799	.00276
.03	.20457	.000077	.90046	.00030	2.6366	.00151	4.7826	.00490
.01	4.9085	.000283	11.536	.00094	16.780	.00255	16.188	.00709

Table 14: $E'_{h,6}$ and $E'_{h,\delta}$ for $f(x) = x^2$

	$N=2000$		$N=1000$		$N=500$		$N=250$	
h	$E'_{h,6}$	$E'_{h,\delta}$	$E'_{h,6}$	$E'_{h,\delta}$	$E'_{h,6}$	$E'_{h,\delta}$	$E'_{h,6}$	$E'_{h,\delta}$
.50	.01676	.02519	.01755	.02645	.01734	.02637	.01967	.02671
.25	.00424	.00656	.00680	.00658	.01538	.00658	.13437	.00683
.12	.00774	.00144	.06827	.00151	.30777	.00153	.93064	.00187
.06	.07000	.00036	.45781	.00040	2.2478	.00074	5.2070	.00175
.03	.81169	.00010	2.9515	.00024	8.8287	.00104	17.062	.00306
.01	17.866	.00016	42.002	.00054	57.692	.00158	59.157	.00429

Table 15: $E'_{h,6}$ and $E'_{h,\delta}$ for $f(x) = e^x$

and

$$T''_{h,\delta}\left(\overline{f}, P''(x_i,h)\right) = \frac{4}{h^3} S(f, P(x_i,h)) - \frac{8}{h^3} S(f, P(x_i, h/2))$$

where

$$\begin{aligned} S(f, P(x_i,h)) = & \left[f(x_m) + \overline{f}(x_i - h)\right](x_m - (x_i - h))/2 \\ & + \sum_{j=m}^{n-1} [f(x_j) + f(x_{j+1})](x_{j+1} - x_j)/2 \\ & + \left[f(x_n) + \overline{f}(x_i + h)\right]((x_i + h) - x_n)/2 \end{aligned}$$

and

$$\begin{aligned} S(f, P(x_i, h/2)) = & \left[f(x_p) + \overline{f}(x_i - h/2)\right](x_p - (x_i - h/2))/2 \\ & + \sum_{j=p}^{q-1} [f(x_j) + f(x_{j+1})](x_{j+1} - x_j)/2 \\ & + \left[f(x_q) + \overline{f}(x_i + h/2)\right]((x_i + h/2) - x_q)/2 \end{aligned}$$

with

$$\overline{f}(x_i - h) = f(x_m) - \frac{[f(x_m) - f(x_{m-1})]}{x_m - x_{m-1}}(x_m - (x_i - h))$$

$$\overline{f}(x_i - h/2) = f(x_p) - \frac{[f(x_p) - f(x_{p-1})]}{x_p - x_{p-1}}(x_p - (x_i - h/2))$$

$$\overline{f}(x_i + h/2) = f(x_q) + \frac{[f(x_{q+1}) - f(x_q)]}{x_{q+1} - x_q}((x_i + h/2) - x_q)$$

$$\overline{f}(x_i + h) = f(x_n) + \frac{[f(x_{n+1}) - f(x_n)]}{x_{n+1} - x_n}((x_i + h) - x_n)$$

and x_m is the first element of $\{x_i\}_{i=1}^N$ in $[x_i - h, x_i + h]$ and x_n is the last while x_p is the first element of $\{x_i\}_{i=1}^N$ in $[x_i - h/2, x_i + h/2]$ and x_q is the last. We then took the average $E''_{h,6}$ of all $e''_{h,6}(f, x_i)$ and the average $E''_{h,\delta}$ of all $e''_{h,\delta}(f, x_i)$ as a measure of the error in approximating f'' by $T''_{h,6}$ and $T''_{h,\delta}$ respectively. The results, are given in Table 16-Table 20.

	$N = 2000$		$N = 1000$		$N = 500$		$N = 250$	
h	$E''_{h,6}$	$E''_{h,\delta}$	$E''_{h,6}$	$E''_{h,\delta}$	$E''_{h,6}$	$E''_{h,\delta}$	$E''_{h,6}$	$E''_{h,\delta}$
.50	.01503	6e-14	.05847	7e-14	.20737	3e-14	.98775	3e-14
.25	.21858	2e-13	.75246	2e-13	3.4114	1e-13	19.453	1e-13
.12	4.1988	2e-12	19.883	2e-12	78.396	1e-12	208.54	1e-12
.06	61.305	4e-12	251.14	4e-12	971.42	3e-12	1995.5	4e-12
.03	920.78	1e-11	2886.9	1e-11	7828.9	1e-11	157402.	1e-11
.01	47942.	9e-11	111513.	8e-11	193204.	6e-11	257824.	6e-11

Table 16: $E''_{h,6}$ and $E''_{h,\delta}$ for $f(x) = 2x + 5$

	$N = 2000$		$N = 1000$		$N = 500$		$N = 250$	
h	$E''_{h,6}$	$E''_{h,\delta}$	$E''_{h,6}$	$E''_{h,\delta}$	$E''_{h,6}$	$E''_{h,\delta}$	$E''_{h,6}$	$E''_{h,\delta}$
.50	628.16	624.56	618.61	615.07	598.60	595.24	583.90	580.76
.25	639.83	652.11	630.05	642.05	609.40	620.64	593.56	603.57
.12	631.65	394.38	357.96	389.66	352.88	382.41	341.50	382.27
.06	116.00	128.33	120.66	128.75	165.33	133.99	246.77	147.35
.03	103.29	35.005	340.49	37.001	941.32	56.923	1833.2	104.01
.01	6327.7	26.641	14180	82.208	23989	257.38	30868	665.13

Table 17: $E''_{h,6}$ and $E''_{h,\delta}$ for $f(x) = \sin(10\pi x)$

	$N = 2000$		$N = 1000$		$N = 500$		$N = 250$	
h	$E''_{h,6}$	$E''_{h,\delta}$	$E''_{h,6}$	$E''_{h,\delta}$	$E''_{h,6}$	$E''_{h,\delta}$	$E''_{h,6}$	$E''_{h,\delta}$
.50	.81720	.91403	.82944	.92780	.80564	.90633	.77843	.88873
.25	.19260	.23934	.15161	.24328	.26032	.23778	2.4921	.22345
.12	.48103	.05572	1.9608	.05615	8.2613	.05953	28.563	.13330
.06	7.7832	.01462	27.407	.02341	121.62	.15326	286.29	.52523
.03	117.75	.02985	330.81	.09363	992.13	.44411	2082.5	1.6909
.01	6226.7	.27869	14093	.7679	23775	2.6371	30716	8.1718

Table 18: $E''_{h,6}$ and $E''_{h,\delta}$ for $f(x) = \sin(\pi x)$

	$N=2000$		$N=1000$		$N=500$		$N=250$	
h	$E''_{h,6}$	$E''_{h,\delta}$	$E''_{h,6}$	$E''_{h,\delta}$	$E''_{h,6}$	$E''_{h,\delta}$	$E''_{h,6}$	$E''_{h,\delta}$
.50	.00178	.00002	.00760	.00007	.02119	.00022	.09696	.00240
.25	.01546	.00006	.05997	.00038	.26778	.00144	1.7848	.01394
.12	.26940	.00039	1.7767	.00243	6.3538	.01220	15.870	.03951
.06	3.8397	.00180	21.011	.00843	66.960	.04492	123.81	.13815
.03	56.647	.00955	204.26	.03531	510.22	.13625	962.70	.49943
.01	3160.8	.08591	7430.7	.26988	12964	.85012	17103	2.4979

Table 19: $E''_{h,6}$ and $E''_{h,\delta}$ for $f(x) = x^2$

	$N=2000$		$N=1000$		$N=500$		$N=250$	
h	$E''_{h,6}$	$E''_{h,\delta}$	$E''_{h,6}$	$E''_{h,\delta}$	$E''_{h,6}$	$E''_{h,\delta}$	$E''_{h,6}$	$E''_{h,\delta}$
.50	.01259	.01886	.00671	.01981	.03795	.01967	.26877	.02008
.25	.04762	.00469	.17563	.00483	.87448	.00474	5.2841	.01273
.12	.97342	.00111	5.3256	.00241	22.118	.01066	51.526	.02448
.06	14.765	.00105	65.430	.00663	253.84	.03425	488.82	.09683
.03	212.60	.00533	706.18	.02345	1883.2	.09219	3600.3	.28659
.01	11044	.04720	25632	.15053	45458	.49424	61898	1.4185

Table 20: $E''_{h,6}$ and $E''_{h,\delta}$ for $f(x) = e^x$

5.3 Using Simpson's rule

We now present results on estimating f'' by the discontinuous kernel $\delta''_{[-h,h]}$ married this time to a quadratic rather than a linear approximation of f (in conjunction with Simpson's rule in place of the trapezoidal rule). If f is three times continuously differentiable and if $x_\alpha, x_\beta, x_\gamma \in \{x_j\}_{j=1}^N$ are three distinct points, then the quadratic approximation formula of Lagrange for f yields

$$\begin{aligned} f_{\alpha,\beta,\gamma}(x) = f(x_\alpha)\frac{(x-x_\beta)(x-x_\gamma)}{(x_\alpha-x_\beta)(x_\alpha-x_\gamma)} + f(x_\beta)\frac{(x-x_\alpha)(x-x_\gamma)}{(x_\beta-x_\alpha)(x_\beta-x_\gamma)} \\ + f(x_\gamma)\frac{(x-x_\alpha)(x-x_\beta)}{(x_\gamma-x_\alpha)(x_\gamma-x_\beta)}. \end{aligned}$$

For any $x_i \in \{x_j\}_{j=1}^N$ we write $x_{i'}$ for the point in $\{x_j\}_{j=1}^{i-1}$ closest to (yet distinct from) x_i and $x_{i''}$ that in $\{x^j\}_{j=i+1}^N$ (when they exist). We then introduce the real function $\widetilde{f}$ on $[x_0-h, x_0+h]$ defined by

$$\widetilde{f}(x) = \begin{cases} f_{m',m,m''}(x) & \text{if } x_0-h \le x < x_{m,m+1} \\ f_{j',j,j''}(x) & \text{if } x_{(j-1),j} \le x < x_{j,(j+1)},\ m<j<n \\ f_{n',n,n''}(x) & \text{if } x_{(n-1),n} \le x \le x_0+h \end{cases}$$

where x_m and x_n are respectively the first and last points of $\{x_j\}_{j=1}^N$ contained in $[x_0-h, x_0+h]$ and

$$x_{i,j} = \frac{x_i+x_j}{2}.$$

Similarly, let x_p and x_q are respectively the first and last points of $\{x_j\}_{j=1}^N$ contained in $[x_0-h/2, x_0+h/2]$. Let us define

$$Q''_{h,\delta}\left(\widetilde{f}, P''(x_0,h)\right) = \frac{4}{h^3}\int_{x_0-h}^{x_0+h}\widetilde{f} - \frac{8}{h^3}\int_{x_0-h/2}^{x_0+h/2}\widetilde{f}$$

where

$$\int_{x_0-h}^{x_0+h}\widetilde{f} = \int_{x_0-h}^{(x_{m-1}+x_m)/2}\widetilde{f} + \sum_{j=m}^{n}\int_{(x_{j-1}+x_j)/2}^{(x_j+x_{j+1})/2}\widetilde{f} + \int_{(x_n+x_{n+1})/2}^{x_0+h}\widetilde{f}$$

and

$$\int_{x_0-h/2}^{x_0+h/2}\widetilde{f} = \int_{x_0-h/2}^{(x_{p-1}+x_p)/2}\widetilde{f} + \sum_{j=p}^{q}\int_{(x_{j-1}+x_j)/2}^{(x_j+x_{j+1})/2}\widetilde{f} + \int_{(x_q+x_{q+1})/2}^{x_0+h/2}\widetilde{f}.$$

To each of the subintegrals we apply Simpson's rule

$$\int_a^b g \approx \frac{(b-a)}{6}\left[g(a) + 4g\left(\frac{a+b}{2}\right) + g(b)\right] \tag{42}$$

(which is precise when g is quadratic on the subintervals, as is the case for $\widetilde{f}$).

The same techniques were applied to the continuous kernel $k = k_{h,\text{poly6}}$. Given a function f three times continuously differentiable, we constructed its quadratic approximation $\widetilde{f}$ via Lagrange's formula. Then f'' which is approximated by $f * k''_{h,\text{poly6}}$, is in turn estimated by $\widetilde{f} * k''_{h,\text{poly6}}$. If we define

$$Q''_{h,6}\left(\widetilde{f}, P(x_0, h)\right) = \left(\widetilde{f} * k''_{h,\text{poly6}}\right)(x_0)$$

then

$$\begin{aligned} Q''_{h,6}\left(\widetilde{f}, P(x_0, h)\right) &= \int_{x_0-h}^{x_0+h} \widetilde{f}(t)\, k''_{h,\text{poly6}}(x_0 - t)\, dt \\ &= \int_{x_0-h}^{(x_{m-1}+x_m)/2} \widetilde{f}(t)\, k''_{h,\text{poly6}}(x_0 - t)\, dt \\ &+ \sum_{j=m}^{n} \int_{(x_{j-1}+x_j)/2}^{(x_j+x_{j+1})/2} \widetilde{f}(t)\, k''_{h,\text{poly6}}(x_0 - t)\, dt \\ &+ \int_{(x_n+x\ln+1)/2}^{x_0+h} \widetilde{f}(t)\, k''_{h,\text{poly6}}(x_0 - t)\, dt \end{aligned}$$

where, by Simpson's rule (42), each subintegral can in turn be approximated by the formula

$$\begin{aligned} \int_a^b \widetilde{f}(t)\, k''(x_0 - t)\, dt \approx\ & \frac{(b-a)}{6}\widetilde{f}(a)\, k''(x_0 - a) \\ &+ 4\frac{(b-a)}{6}\widetilde{f}\left(\frac{a+b}{2}\right) k''\left(x_0 - \frac{a+b}{2}\right) \\ &+ \frac{(b-a)}{6}\widetilde{f}(b)\, k''(x_0 - b)\,. \end{aligned}$$

For each N, h and $x_i \in [-1, 1]$ we calculated the errors

$$\text{qde}''_{h,6}(f, x_i) = \left| f''(x_i) - Q''_{h,6}\left(\widetilde{f}, P(x_i, h)\right)\right|$$

	$N=2000$		$N=1000$		$N=500$		$N=250$	
h	$\mathrm{qd}E''_{h,6}$	$\mathrm{qd}E''_{h,\delta}$	$\mathrm{qd}E''_{h,6}$	$\mathrm{qd}E''_{h,\delta}$	$\mathrm{qd}E''_{h,6}$	$\mathrm{qd}E''_{h,\delta}$	$\mathrm{qd}E''_{h,6}$	$\mathrm{qd}E''_{h,\delta}$
.50	.06217	1e-13	.19007	6e-14	.67015	3e-14	1.8283	3e-14
.25	.65550	2e-13	2.6961	2e-13	11.123	1e-13	29.328	1e-13
.12	11.021	2e-12	42.201	2e-12	133.67	1e-12	247.62	1e-12
.06	132.22	4e-12	487.25	4e-12	1251.4	4e-12	1763.6	5e-12
.03	1709.4	1e-11	4325.5	1e-11	7515.9	1e-11	9887.5	3e-11
.01	56643	1e-10	82555	9e-11	107792	1e-10	147700	5e-10

Table 21: $\mathrm{qd}E''_{h,6}$ and $\mathrm{qd}E''_{h,\delta}$ for $f(x) = 2x + 5$

	$N=2000$		$N=1000$		$N=500$		$N=250$	
h	$\mathrm{qd}E''_{h,6}$	$\mathrm{qd}E''_{h,\delta}$	$\mathrm{qd}E''_{h,6}$	$\mathrm{qd}E''_{h,\delta}$	$\mathrm{qd}E''_{h,6}$	$\mathrm{qd}E''_{h,\delta}$	$\mathrm{qd}E''_{h,6}$	$\mathrm{qd}E''_{h,\delta}$
.50	628.50	624.56	618.97	615.06	599.11	595.21	584.49	580.53
.25	644.05	652.15	634.20	642.24	613.64	621.52	596.88	606.49
.12	273.05	393.99	272.72	387.99	273.40	375.17	285.80	362.03
.06	55.004	127.49	67.385	125.54	135.55	122.25	239.31	130.59
.03	318.57	34.099	606.71	33.918	966.72	37.702	1205.4	70.362
.01	7400.9	4.8847	10382	11.231	13316	28.024	19328	77.686

Table 22: $\mathrm{qd}E''_{h6}$ and $\mathrm{qd}E''_{h,\delta}$ for $f(x) = \sin(10\pi x)$

and

$$\mathrm{qde}''_{h,\delta}(f, x_i) = \left| f''(x_i) - Q''_{h,\delta}\left(\widetilde{f}, P''(x_i, h)\right)\right|.$$

We then took the average $\mathrm{qd}E''_{h,6}$ of all $\mathrm{qde}''_{h,6}(f, x_i)$ and the average $\mathrm{qd}E''_{h,\delta}$ of all $\mathrm{qde}''_{h,\delta}(f, x_i)$ as a measure of the error in approximating $f''(x_i)$ by $Q''_{h,6}\left(\widetilde{f}, P(x_i, h)\right)$ and $Q''_{h,\delta}\left(\widetilde{f}, P''(x_i, h)\right)$ respectively. The results are given in Table 21 -Table 25.

6 Conclusion

We introduced, for arbitrary $h > 0$, discontinuous kernels (12), (16) and (20) with support in $[-h, h]$ such that their convolution with a given function f yields an approximation of the function, along with its first and second derivatives, respectively. It was shown that such an approximation is subject to an error of order $O(h^2)$. Since the values of f are assumed known

	$N=2000$		$N=1000$		$N=500$		$N=250$	
h	qd$E''_{h,6}$	qd$E''_{h,\delta}$	qd$E''_{h,6}$	qd$E''_{h,\delta}$	qd$E''_{h,6}$	qd$E''_{h,\delta}$	qd$E''_{h,6}$	qd$E''_{h,\delta}$
.50	1.0108	.91392	1.0255	.92741	.99686	.90490	.99755	.88394
.25	1.8582	.23925	2.0685	.24278	2.6724	.23689	4.5225	.23151
.12	2.9782	.05578	6.2623	.05661	17.439	.05527	31.901	.05423
.06	17.746	.01398	61.854	.01420	152.75	.01488	229.71	.02583
.03	215.91	.00349	511.98	.00483	930.64	.01363	1148.5	.03819
.01	7263.5	.00222	10340	.01007	13059	.02758	17496	.06921

Table 23: qd$E''_{h,6}$ and qd$E''_{h,\delta}$ for $f(x)=\sin(\pi x)$

	$N=2000$		$N=1000$		$N=500$		$N=250$	
h	qd$E''_{h,6}$	qd$E''_{h,\delta}$	qd$E''_{h,6}$	qd$E''_{h,\delta}$	qd$E''_{h,6}$	qd$E''_{h,\delta}$	qd$E''_{h,6}$	qd$E''_{h,\delta}$
.50	.66174	7e-15	.65222	5e-15	.59945	5e-15	.54680	3e-15
.25	.63059	2e-14	.57494	1e-14	.95113	1e-14	2.3073	9e-15
.12	.89221	1e-13	3.2750	1e-13	10.710	1e-13	17.376	1e-13
.06	9.0254	2e-13	34.967	2e-13	79.066	2e-13	109.71	2e-13
.03	112.91	1e-12	285.38	1e-12	477.69	1e-12	607.18	1e-12
.01	3907.8	8e-12	5409.8	7e-12	7332.3	7e-12	9811.5	2e-11

Table 24: qd$E''_{h,6}$and qd$E''_{h,\delta}$ for $f(x)=x^2$

	$N=2000$		$N=1000$		$N=500$		$N=250$	
h	qd$E''_{h,6}$	qd$E''_{h,\delta}$	qd$E''_{h,6}$	qd$E''_{h,\delta}$	qd$E''_{h,6}$	qd$E''_{h,\delta}$	qd$E''_{h,6}$	qd$E''_{h,\delta}$
.50	.41096	.01825	.40421	.01979	.26527	.01971	.35892	.01986
.25	.29629	.00469	.56251	.00492	2.8432	.00490	7.9090	.00495
.12	2.5358	.00108	10.535	.00113	35.835	.00115	60.577	.00139
.06	31.271	.00027	118.83	.00029	310.40	.00044	422.52	.00164
.03	402.65	.00007	1052.3	.00016	1834.5	.00083	2403.2	.00285
.01	13333	.00011	19877	.00059	25765	.00175	35259	.00454

Table 25: qd$E''_{h,6}$ and qd$E''_{h,\delta}$ for $f(x)=e^x$

only on a finite set of points, (denoted by the ordered sequence $\{x_j\}_{j=1}^{N}$) we further approximated the convolutions by numerical methods based on the trapezoidal rule applied to a linear approximation of f. In the case of the second derivative, we also used Simpson's rule applied to a quadratic approximation of f. In so doing, we obtained for $h > 0$ small enough a significant improvement in the estimates when compared with the classic methods of SPH. In fact, our methods were more accurate and numerically stable than those based on classic SPH for small h and/or N. Furthermore, Simpson's rule proved to be significantly better than the trapezoidal rule in estimating a second derivative as h got smaller. When the same techniques were applied to the smooth kernel $k_{h,\text{poly6}}$ given by (8) (and its derivatives) in place of our discontinuous kernels (12), (16) and (20), we obtained numerical results for small h and/or N no better than those obtained by classic SPH. This justifies, for small h and/or N, the use of discontinuous kernels like (12), (16) and (20) over continuous kernels, when used in conjunction with a Newton-Cotes integration formula of which the trapezoidal rule and Simpson's rule are the most elementary.

In this paper we gave bounds for approximations based on SPH techniques. We showed that when f is twice continuously differentiable, and when $|x_j - x_{j-1}| < h$ for $j = 2, ..., N$, then the error in approximating f by the trapezoidal rule in conjunction with a linear approximation of f is of order $O(h^2)$. The same result was obtained for the derivative whenever f is three times continuously differentiable, and for the second derivative whenever f is four times continuously differentiable.

Even though the extension of the discontinuous kernels to the multi-dimensional case can be easily derived from the one-dimensional case, there are still some problems to overcome regarding the definition of simple and elegant sums satisfying the discrete reproducing conditions. For this reason, it remains our aim to study discontinuous kernels in the multi-dimensional setting.

Acknowledgement. *We wish to express our gratitude to John Yawney for his independent numerical calculations that corroborated ours.*

References

[1] K.E. Atkinson. An Introduction to Numerical Analysis. John Wiley & Sons, 1978.

[2] M. Desbrun and M.P. Cani. Smoothed particles: A new paradigm for animating highly deformable bodies. *Computer Animation and Simulation '96 (Proceedings of EG Workshop on Animation and Simulation),* 61-76. Springer-Verlag, Aug 1996.

[3] R. Capuzzo-Dolcetta and R. Di Lisio. A criterion for the choice of the interpolation kernel in smoothed particle hydrodynamics. *Appl. Numer. Math.* 34 (2000) 363-371.

[4] M. Carlson, P.J. Mucha, R.B. Van Horn et G. Turk. Melting and flowing. *Proceedings of the ACM SIGGRAPH symposium on Computer animation,* pages 167-174, ACM Press, 2002.

[5] M. Ellero, M. Kröger and S. Hess. Viscoelastic flows studied by smoothed particle dynamics. *J. Non-Newtonian Fluid Mech.* 105 (2002) 35-51.

[6] D. Enright, S. Marschner and R. Fedkiw. Animation and rendering of complex water surfaces. *Proceedings of the 29^{th} annual conference on Computer graphics and interactive techniques*, pages 736-744, ACM Press, 2002.

[7] N. Foster and R. Fedkiw. Practical animation of liquids. *Proceedings of the 28^{th} annual conference on Computer graphics and interactive techniques*, pages 23-30, ACM Press, 2001.

[8] R.A. Gingold and J.J. Monaghan. Smoothed particle hydrodynamics: theory and application to non-spherical stars. *Monthly Notices Roy. Astron. Soc., 181 (1977) 375-398.*

[9] D. Hinsinger, F. Neyret and M-P. Cani. Interactive animation of ocean waves. *Proceedings of the ACM SIGGRAPH symposium on Computer animation,* pages 161-166, ACM Press, 2002.

[10] G.R. Liu and M.B. Liu. Smoothed Particle Hydrodynamics, a mesh free particle method. World Scientific Publishing Co. Pte. Ltd., Singapore 2003.

[11] M.B. Liu, G.R. Liu and K.Y. Lam. Constructing smoothing functions in smoothed particle hydrodynamics with applications. *Journal of Computational and Applied Mathematics* 155 (2003) 263-284.

[12] L.B. Lucy. A numerical approach to the testing of the fission hypothesis. *Astronom. J.,* 82 (1977) 1013-1024.

[13] J.J. Monaghan. Simulating free surface flow with SPH, *J. Comput. Phys.*, 110 (1994) 399-406.

[14] Matthias Müller, David Charypar and Markus Gross. Particle-Based Fluid Simulation for Interactive Applications. *Proceedings of the ACM SIGGRAPH symposium on Computer animation,* pages 154-159, ACM Press, 2003.

[15] D. Nixon and R. Lobb. A fluid-based soft-object model. *IEEE CG&A, (*July/August 2002) 68-75.

[16] D. Stora, P-O. Agliati, M-P. Cani, F. Neyret and J-D. Gascuel. Animating lava flows. *Graphics Interface,* (1999) 203-210.

CONCLUSION

Nous avons introduit trois noyaux discontinus avec support $[-h, h]$, où $h > 0$, tels que la convolution d'une fonction f avec ces noyaux fournisse une approximation de la valeur de la fonction ainsi que de ses dérivées première et seconde, respectivement. On a montré que, dans ces trois cas, l'erreur obtenue par la convolution est d'ordre $O(h^2)$. Puisque les valeurs de f ne sont connues qu'en un nombre fini de points (représentés par la suite ordonnée $\{x_j\}_{j=1}^N$), on a ensuite approximé les convolutions à l'aide des méthodes numériques basées sur la règle du trapèze et l'approximation linéaire de la fonction. On a montré que lorsque f est deux fois continûment différentiable, et lorsque $|x_j - x_{j-1}| < h$ pour $j = 2, ..., N$, alors l'erreur commise en utilisant la règle du trapèze avec l'approximation linéaire est aussi d'ordre $O(h^2)$. Nous avons obtenu le même résultat pour la dérivée d'une fonction trois fois continûment différentiable, et pour la dérivée second lorsque la fonction est quatre fois continûment différentiable. Dans le cas de la dérivée seconde, on a aussi estimé la convolution à l'aide de la règle de Simpson et de l'approximation quadratique de la fonction. Comparativement à la méthode SPH classique, nous avons constaté une grande amélioration des approximations. Lorsque h et N sont petits, nos méthodes sont plus précises. (En SPH classique, pour que la précision augmente lorsque h devient petit, il faut que N augmente.) De plus, la règle de Simpson s'est révélée beaucoup plus précise que celle basée sur la méthode du trapèze lorsque h décroissait. Lorsque les mêmes techniques sont appliquées au noyau $k_{h,\text{poly6}}$ (et à ses dérivées) à la place des noyaux discontinus que nous proposons, nous obtenons des résultats numériques qui n'offrent aucun avantage sur les méthodes classiques

SPH dans le cas de petits h et petits N. Ces faits justifient, pour de petites valeurs de h et de N, l'emploi de nos noyaux discontinus dans le calcul de la valeur d'une fonction et de ses deux premières dérivées en un point.

BIBLIOGRAPHIE

[DESB96] M. Desbrun and M.P. Cani. Smoothed particles: A new paradigm for animating highly deformable bodies. *Computer Animation and Simulation '96 (Proceedings of EG Workshop on Animation and Simulation)*, 61-76. Springer-Verlag, Aug 1996.

[CAPU00] R. Capuzzo-Dolcetta and R. Di Lisio. A criterion for the choice of the interpolation kernel in smoothed particle hydrodynamics. *Appl. Numer. Math.* 34 (2000) 363-371.

[CARL02] M. Carlson, P.J. Mucha, R.B. Van Horn et G. Turk. Melting and flowing. *Proceedings of the ACM SIGGRAPH symposium on Computer animation,* pages 167-174, ACM Press, 2002.

[DOBR81] B.M. Dobratz. LLNL Explosive Handbook, UCRL-52997, Lawrence Livermore National Laboratory, Livermore, CA., 1981.

[ELLE02] M. Ellero, M. Kröger and S. Hess. Viscoelastic flows studied by smoothed particle dynamics. *J. Non-Newtonian Fluid Mech.* 105 (2002) 35-51.

[ENRI02] D. Enright, S. Marschner and R. Fedkiw. Animation and rendering of complex water surfaces. *Proceedings of the 29th annual conference on Computer graphics and interactive techniques,* pages 736-744, ACM Press, 2002.

[FOST01] N. Foster and R. Fedkiw. Practical animation of liquids. *Proceedings of the 28^{th} annual conference on Computer graphics and interactive techniques*, pages 23-30, ACM Press, 2001.

[GING77] R.A. Gingold and J.J. Monaghan. Smoothed particle hydrodynamics: theory and application to non-spherical stars. *Monthly Notices Roy. Astron. Soc., 181 (1977) 375-398.*

[HINS02] D. Hinsinger, F. Neyret and M-P. Cani. Interactive animation of ocean waves. *Proceedings of the ACM SIGGRAPH symposium on Computer animation,* pages 161-166, ACM Press, 2002.

[LIUL03a] G.R. Liu and M.B. Liu. Smoothed Particle Hydrodynamics, a mesh free particle method. World Scientific Publishing Co. Pte. Ltd., Singapore 2003.

[LIUL03b] M.B. Liu, G.R. Liu and K.Y. Lam. Constructing smoothing functions in smoothed particle hydrodynamics with applications. *J. Comput. Appl. Math.* 155 (2003) 263-284.

[LUCY77] L.B. Lucy. A numerical approach to the testing of the fission hypothesis. *Astronom. J.,* 82 (1977) 1013-1024.

[MULL03] Matthias Müller, David Charypar and Markus Gross. Particle-Based Fluid Simulation for Interactive Applications. *Proceedings of the ACM SIGGRAPH symposium on Computer animation,* pages 154-159, ACM Press, 2003.

[NIXO02] D. Nixon and R. Lobb. A fluid-based soft-object model. *IEEE CG&A, (*July/August 2002) 68-75.

[SCHL99] B. Schlatter. Modeling fluid flow using smoothed particle hydrodynamics, Masters Thesis, Oregon State University 1999.

[STOR99] D. Stora, P-O. Agliati, M-P. Cani, F. Neyret and J-D. Gascuel. Animating lava flows. *Graphics Interface,* (1999) 203-210.